Available online at www.sciencedirect.com
SCIENCE DIRECT®
Journal of Organometallic Chemistry 689 (2004) 4016–4054
Journal of Organometallic Chemistry
www.elsevier.com/locate/jorganchem

Review

Where organometallics and dendrimers merge: the incorporation of organometallic species into dendritic molecules

Preston A. Chase, Robertus J.M. Klein Gebbink [1], Gerard van Koten *

Debye Institute, Department of Metal-Mediated Synthesis, Utrecht University, Padualaan 8, 3584 CH Utrecht, The Netherlands

Received 14 June 2004; accepted 15 July 2004
Available online 23 August 2004

Abstract

This review will describe the ongoing efforts being made to incorporate organometallic fragments into the framework of dendrimers. While purely dendritic organic molecules are well known and well studied, species incorporating organometallic moieties potentially offer many benefits that are not available to only organic containing dendrimers. For example, catalytic or redox active organometallic functions can be included in the dendritic framework and impart these characteristics onto the dendrimer. This report will give an overview of the latest developments in this field by highlighting selected examples that detail novel synthetic strategies or dendrimer construction methodologies, interesting practical applications or address specific problems associated with organometallic dendrimers.

Keywords: Dendrimers; Organometallics; Review; Synthesis; Applications

1. Introduction

Dendrimers are large, mono-disperse, highly/hyper branched molecules with precisely designed and defined structures. Since their initial conceptual development, the research and practical applications of dendritic materials has blossomed [1,2]. While most of the dendrimers synthesized to date are organic molecules [3], there has been significant effort put forward towards the incorporation of other main group elements [4], and organometallic or transition metal entities and fragments [5,6]. This merging of fields hopes to combine the properties of the organometallic or transition metal species, such as catalytic [7–9], electrochemical, optical and magnetic properties, with the benefits generally attributed to dendrimers, such as site isolation [10,11], precise steric environments, recyclability [12] and possible cooperative effects. This topic has intrigued and excited numerous groups and has resulted in a myriad of new structures and architectures as well as applications for these species.

Reported in 1994 by Puddephatt, a dendrimer was constructed in which an organometallic species, incorporating a Pt^{IV} center, was used as an integral structural feature [13,14]. This was the first example of a dendrimer where an organometallic fragment was incorporated into every generation. In general, one of the long-standing problems in dendrimer synthesis for both organic and organometallic species is the discovery of high yielding, selective reactions that allow the dendrimers to be synthesized without defects, for example, the incomplete substitution of the reactive groups in the periphery. Puddephatt employed two reactions of Pt^{II} that here known to be essentially quantitative: (1) the oxidative addition of a benzylic bromide to a 2,2′-bipyridine

* Corresponding author. Tel.: +31 30 2533120; fax: +31 30 2523615.
E-mail addresses: r.j.m.kleingebbink@chem.uu.nl (Robertus J.M. Klein Gebbink), g.vankoten@chem.uu.nl (G. van Koten).
URL: http://www.chem.uu.nl/soc.
[1] Tel.: +31 30 2531889; fax: +31 30 2523615.

0022-328X/$ - see front matter © 2004 Elsevier B.V. All rights reserved.
doi:10.1016/j.jorganchem.2004.07.032

(bipy) dimethyl Pt center and (2) the ligand displacement of bound SMe_2 groups with the chelating bipy ligand. By incorporation of a benzylic bromide in substituted bipy compounds, the fabrication of organometallic dendrimers was achieved. The reaction sequence for the initial stages of dendrimer formation is shown in Scheme 1. This cycle was repeated three times to generate a second generation dendrimer **1**, depicted in Fig. 1. Further reactions to obtain higher generations were unsuccessful [15] but this study was the first to show that reactions involving organometallic species could be employed to generate dendritic structures in which metal centers were integrated into the dendrimer skeleton.

One of the first organometallic dendrimers to be applied in catalysis was reported by the groups of van Koten and van Leeuwen [16]. The periphery of a carbosilane (CS) dendrimer was adorned with terdentate monoanionic aryl diamino "NCN" pincer supported nickel groups. Zeroth and first generation dendrimers, $\mathbf{G_0}\mathbf{2}$ and $\mathbf{G_1}\mathbf{2}$, respectively, were constructed via a divergent route and the pincer function was introduced by reaction of the peripheral Me_2SiCl groups in the dendrimer with a pincer containing a terminal alcohol in the presence of NEt_3 base. The structures are shown in Fig. 2. This dendrimer was applied as a homogeneous catalyst for the Kharasch addition of polyhaloalkanes to alkenes. The activity of the dendrimer was only slightly less than that of the monomeric species (82 and 71% for $\mathbf{G_0}\mathbf{2}$ and $\mathbf{G_1}\mathbf{2}$, respectively) and most likely arises from incomplete Ni incorporation. The yields of the reaction were based on quantitative metallation of the dendrimer, but, in the case of $\mathbf{G_1}\mathbf{2}$ for example, the average incorporation was found to be 11 nickel centers. The products produced by the dendritic catalyst were identical to the monomeric systems. This indicated that incorporation of a catalytically active metal into a dendritic structure allowed for similar reactivity to occur on a dendrimer surface as in solution. While not tested in the original publication, the CS-dendrimer-supported pincer catalysts can be removed from a reaction mixture via ultrafiltration (vide infra). This report helped to set the stage for the practical application of dendrimers to address specific deficiencies in homogeneous catalysis, for this system, the removal and reuse of the catalyst.

From these auspicious beginnings, research on the incorporation of organometallic species and fragments into the framework of a dendrimer has exhibited phenomenal growth. This is indeed a vast field and, in this review, we will focus on dendrimers that incorporate an organometallic moiety as an integral structural feature of the dendrimer framework. Due to the breadth of the body of research that has been reported, we will focus on dendrimers with strictly organometallic linkages between the metal and the dendrimer framework, i.e., a σ or π metal–carbon bond. This will exclude coordination compounds in which the dendrimer and metal are linked through a dative metal–heteroatom bond [17] and also dendrimers interdispersed with metal nanoparticles [18,19] Also, we will not incorporate strictly main group or main group organometallic dendrimers in this review [4]. The reader is directed to the previously mentioned reviews and books for further information on these topics. In addition to these, a small number of reviews have detailed the research on dendrimers containing organometallic or transition metal moieties [5,6]. These reviews cover most of the major results in the field of organometallic dendrimers prior to 1999. As such, we will focus on the developments in the field after this time. Some other reviews have appeared [7–9,20] but do not strictly focus on organometallic dendrimers, as defined here. While this report is not intended to be comprehensive, our aim is to give an overview of the field and highlight specific examples that illustrate general synthetic strategies or particularly useful reactions as well as the utility and application of these interesting dendrimers.

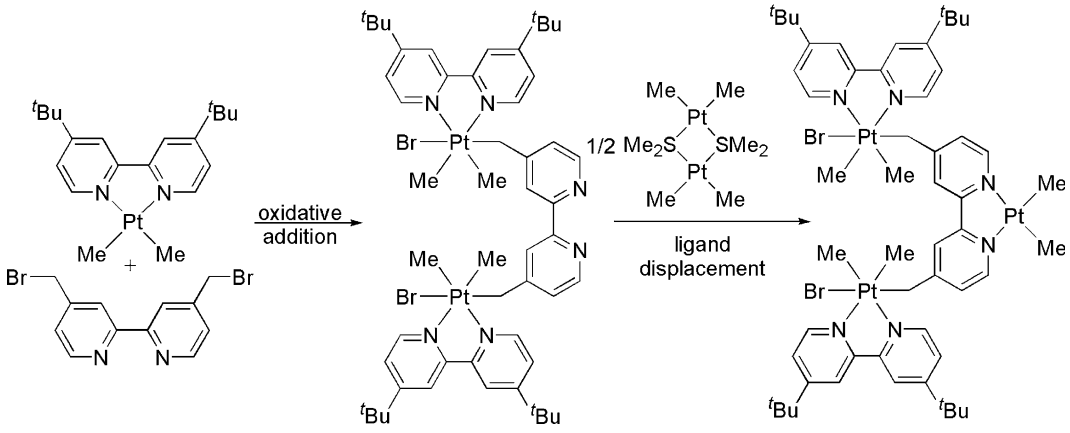

Scheme 1. Synthetic methodology for generation of Puddephatt's Pt(bipy) dendrimers.

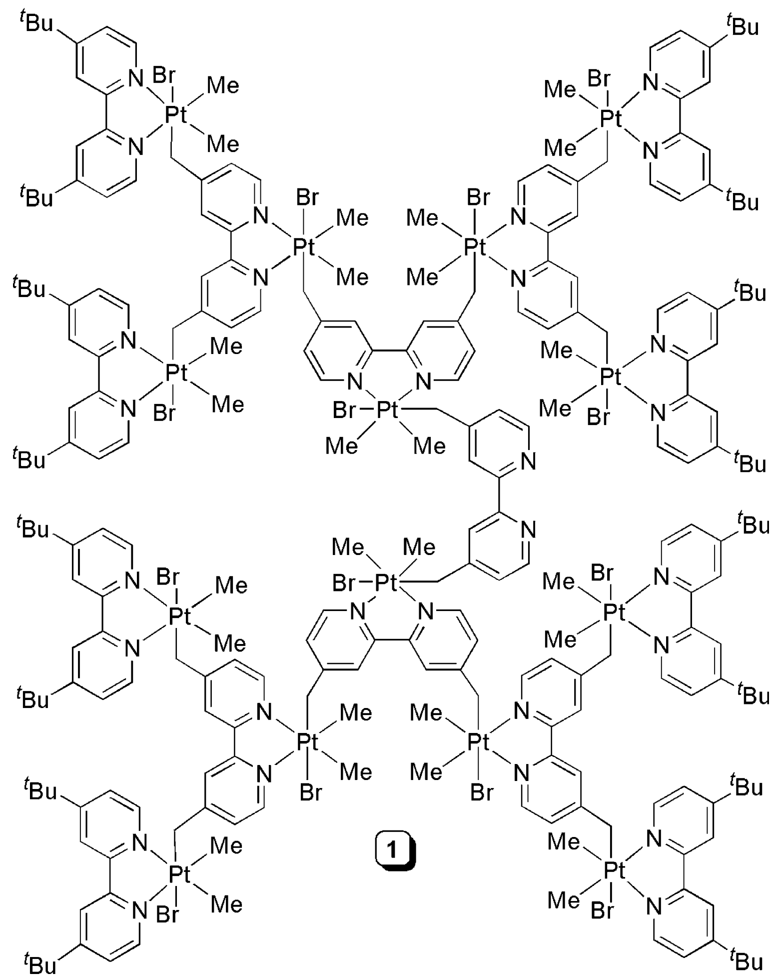

Fig. 1. Structure of Puddephatt's second generation Pt(bipy) dendrimer **1**.

The presentation of the research described herein will be delineated by the position of the organometallic species in the dendrimer framework: on the periphery, within the dendrimer core, and throughout the dendrimer backbone. Due to the number of dendrimers in which a ferrocene group is peripherally substituted, these compounds will be presented in a separate subsection within this grouping. The focus will be on the synthetic methodologies for incorporation of the organometallic unit into the dendrimer and on the structure and intrinsic physical or spectroscopic properties of the organometallic containing species. Also, demonstrated or potential applications of the organometallic containing dendrimers will be highlighted.

2. Peripheral substitution of dendrimers with organometallic species

Dendrimers with organometallic functionalities decorating the periphery are, by far, the most common of this type of organometallic containing dendrimer species. Often the methodologies for construction of the dendrimer framework have been previously elucidated for a specific transition metal and, for other organometallic fragments, have been successfully transposed for the new metal. Alternatively, the simple dendrimer is commercially available, such as the diamino butane (DAB), poly(amido)amine (PAMAM), or Newkome-type dendrimers, and only final modifications to the peripheral functional groups and/or introduction of the organometallic fragment need to be performed. As such, these dendrimers tend to be fashioned with a specific function or goal in mind, such as incorporation of a catalytic site or redox active center. The merging of the potential properties of dendrimers with demonstrated functionality of an organometallic species was identified early on as a worthy and potentially lucrative goal.

2.1. Ferrocenyl substituted in the periphery of dendrimers

Due to their high degree of chemical and thermal stability as well as thoroughly investigated and well-understood electrochemical properties, there have been

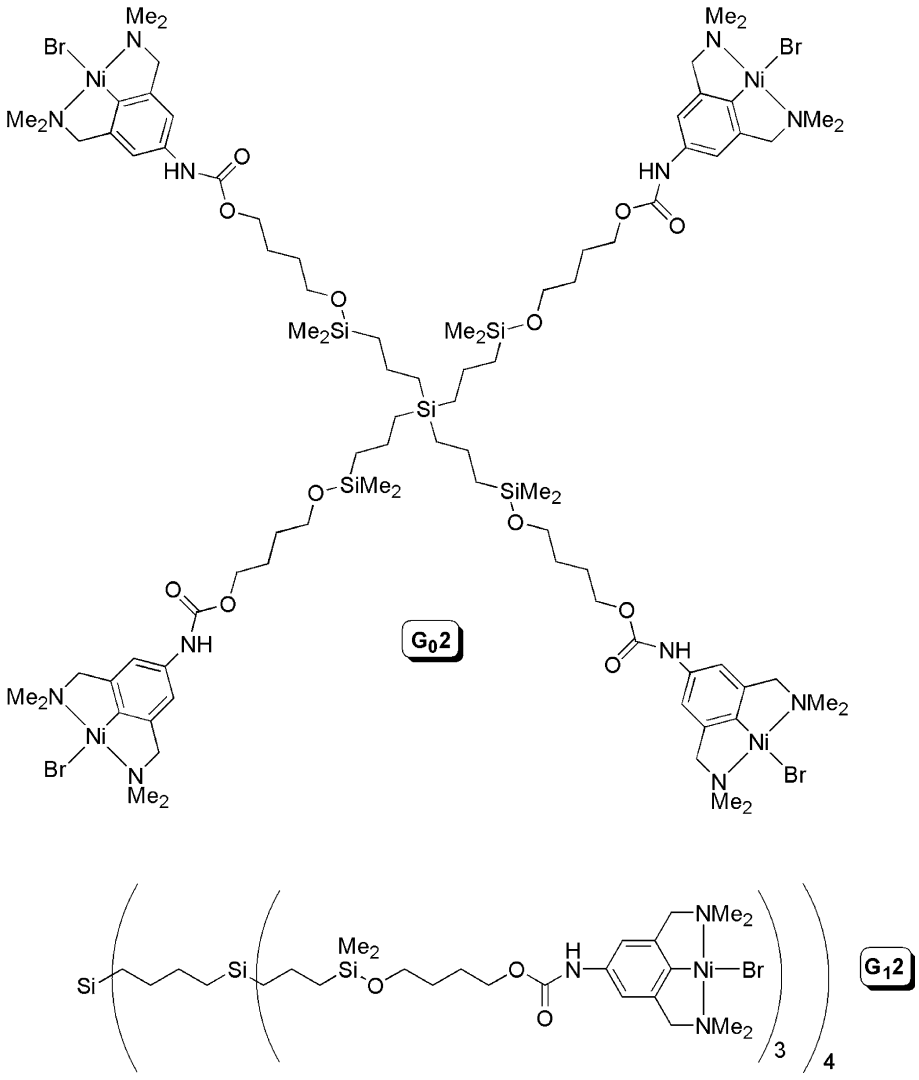

Fig. 2. Structure of van Koten's carbosilane pincer nickel dendrimers **2**.

many reports on the introduction of ferrocene units on the periphery of dendrimers. The main aspects of this work prior to 1999 have been reviewed by Moss [5] and by Cuadrado [6]. While much of the groundwork has been laid in this specific field, many publications are still focusing on this area which extend the understanding of the interaction of the dendrimer with both the incorporated ferrocene group and other outside species, such as electrode surfaces or solutes.

Much of the work in this field has progressed beyond simple synthesis of novel structures or compounds and has been extended into practical applications. Most of the uses for these ferrocenyl systems exploit their well-studied redox behavior and some speciality devices have been fashioned in which electrodes with dendrimer coatings for redox sensing of analytes have been built. Some recent reports have included the electrochemical sensing of bio-relevant molecules, such as biotin, DNA, nucleic acids and carbohydrates using electrodes incorporating dendrimers of ferrocene along with a specific analyte binding function [21,22].

While many architectures for the core and arms of the dendrimer have been employed, the most common being poly(amine), amides, carbosilane or Fréchet-type benzylic ether scaffolds, some new methodologies have recently been introduced with the potential to alter the properties and applications of the functional groups or to add extra degrees of flexibility in the systems. Astruc and coworkers have employed non-covalent hydrogen bonding as a synthetic pathway to construct a dendrimer containing ferrocene groups [23]. The use of H-bonding for dendrimer construction has been previously employed [10,24,25] but this is the first instance using this methodology to incorporate an organometallic fragment. With commercially available DAB polyamine dendrimers of generations 1-4 and dendrons containing three ferrocenyl and a single phenolic unit (**3**), N–H–O bonding interactions were used to generate the

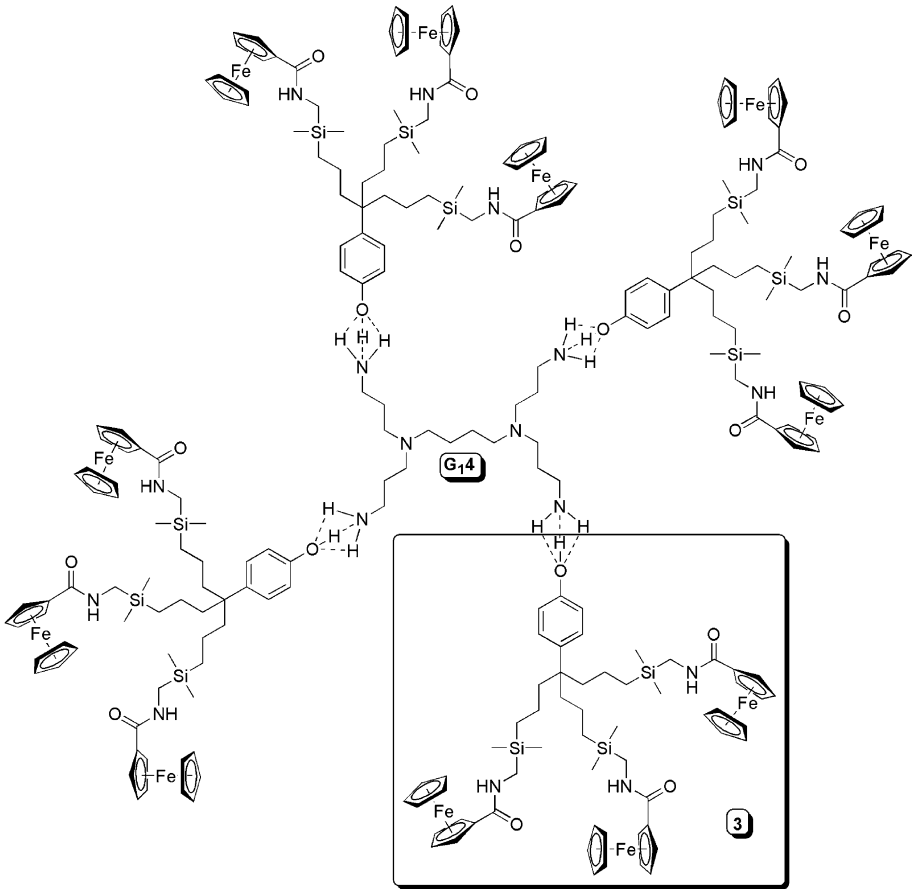

Fig. 3. Structure of Astruc's H-bonded dendrimer $\mathbf{G_1 4}$.

dendrimer assembly. A depiction of the first generation dendrimer $\mathbf{G_1 4}$ is shown in Fig. 3. Evidence for formation of the H-bonding interactions was established by NMR experiments. The ^{1}H NMR signals for both the NH_2 and ArOH protons ($\delta = 1.5$ and 5.0, respectively, for the free species) are broadened and shifted to a single, broad resonance at $\delta = 2.4$–4.1, indicating interaction between these functional groups and evidence for hydrogen bonding.

These dendrimer assemblies were used in the recognition of $H_2PO_4^-$ anions, which was probed by cyclic voltametry (CV) studies. As previously investigated by Astruc [26], the addition of $H_2PO_4^-$ to an amido-substituted ferrocene, FcC(O)NHPr, resulted in a decrease in intensity of the initial wave and the appearance of a new wave at less positive potential. Upon reaching a 1:1 stoichiometry, the initial wave disappears. The value for the change in potential of the $Fc^{II/III}$ waves, $\Delta E_{1/2}$, in the absence and with one equivalent of $H_2PO_4^-$, was found to be 150 mV. To determine if the incorporation of the amidoferrocene group in a dendritic system has an effect, a control experiment using the phenolic dendron **3** and *n*-propylamine ($PrNH_2$) was performed and the $\Delta E_{1/2}$ value was found to be 205 mV. Using both the ferrocenyl-substituted $\mathbf{G_1 4}$ and $\mathbf{G_2 4}$ DAB dendrimers resulted in an increase in the value of $\Delta E_{1/2}$ to 250 and 280 mV, respectively. This increase indicates that there is a difference in $\Delta E_{1/2}$ upon introduction of the dendrimer with respect to the monomeric system and that H-bonding interactions generating dendritic species are present under these conditions. In this case, this is a positive dendritic effect. The larger $\mathbf{G_3 4}$ and $\mathbf{G_4 4}$ DAB systems gave results identical to that of the $\mathbf{G_2 4}$ dendrimer, indicating that saturation has already occurred at the second generation. In addition to the effect on the $\Delta E_{1/2}$ values, there was a large difference in the amount of $H_2PO_4^-$ needed to reach the equivalence point between the $PrNH_2$ system and the DAB dendrimers. In the case of $PrNH_2$, 2.5 equivalents of $H_2PO_4^-$ were needed per dendritic branch, presumably due to competitive H-bonding between the added amine and **3** for $H_2PO_4^-$. For the DAB dendrimers, the equivalence point is reached with 0.5, 0.8, 2.0 and 2.0 equivalents for the $\mathbf{G_1 4}$, $\mathbf{G_2 4}$, $\mathbf{G_3 4}$ and $\mathbf{G_4 4}$ dendrimers, respectively. The significant drop comparing the $PrNH_2$ system to the G_1 dendrimer is proposed to be the result of restricted access of the $H_2PO_4^-$ anion to the sterically more congested amines of the DAB molecules and points to chelation by the amidoferrocene units. The increase with higher generation dendrimers is due to steric congestion

on the surface and to possible disruption of H-bonding, which is consistent with the $\Delta E_{1/2}$ results. With the **G$_1$4** system, the precise 0.5 equivalents necessary to reach the equivalence point is consistent with a structure in which each of the $H_2PO_4^-$ anions is binding with two aminoferrocenes, also by H-bonding, generating the complexed dendrimer **G$_1$4**·$H_2PO_4^-$ shown in Fig. 4. The complex also contains six [nBu$_4$N] counterions. This structure should incorporate, based on the stoichiometry, two separate H-bonding motifs for interaction of the $H_2PO_4^-$ anion. The first is between two amido C=O groups of the amidoferrocenes within the same dendron arm with one $H_2PO_4^-$ and the other employs amidoferrocenes from adjacent dendron arms to chelate the other $H_2PO_4^-$ anion. While this is likely a fluxional process, the electrochemical data does indication that this type of structure does exist on the time scale of the electrochemical experiment and that there is no interdendritic bridging by the $H_2PO_4^-$ anion.

Majoral and coworkers have employed phosphorus containing dendrimers [6,27] to study the effect of the position of a chiral ferrocene within the dendrimer structure on its chiroptical and electrochemical properties [28]. Dendrimers were synthesized in which the ferrocene unit was sequentially ensconced within successive dendrimer generations. To investigate the effect of "burying" the electroactive organometallic functionality, the known phosphorus-containing dendrimers of Majoral were used and ferrocenyl aldehyde endgroups were incorporated, which have planar chirality [29]. Additional dendrimer layers were added via condensation of a phosphorhydrazide $H_2NNMeP(S)Cl_2$ and subsequent reaction with two equivalents of 4-hydroxybenzaldehyde sodium salt and the pendant PCl_2 group as shown in Scheme 2. All of the reaction steps were quite high yielding (>85%) and dendrimers out to the eleventh generation were synthesized.

Initially, ferrocenyl-substituted phosphorus-containing dendrimers of third, fifth and ninth generation of dendrimers **5** were employed and the metallocene was capped (**6**) and buried within additional first and second dendritic generations (**G$_{3+1}$6** or **G$_{3+2}$6**), respectively. Scheme 2 depicts the synthesis of the third generation dendrimer **G$_3$6** and additional layers to generate **G$_{3+1}$6** and **G$_{3+2}$6**. The reactions were monitored and the dendrimers were characterized via multinuclear NMR

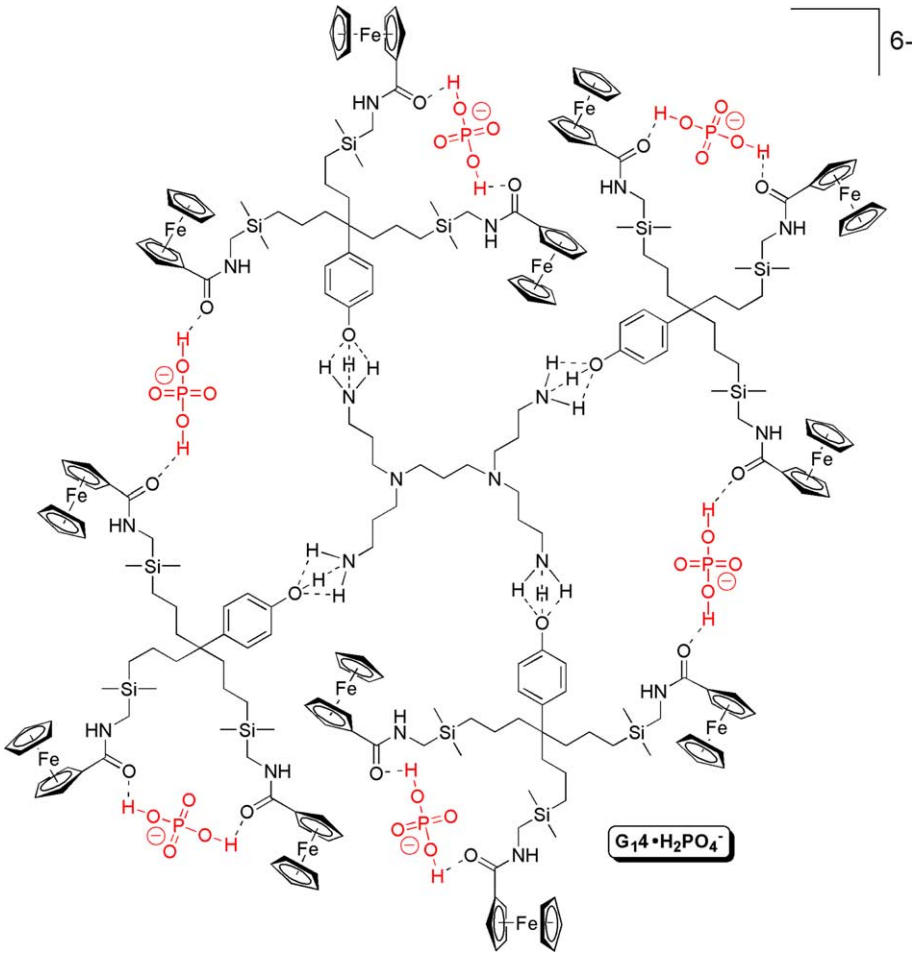

Fig. 4. Proposed structure of Astruc's **G$_1$4**·$H_2PO_4^-$.

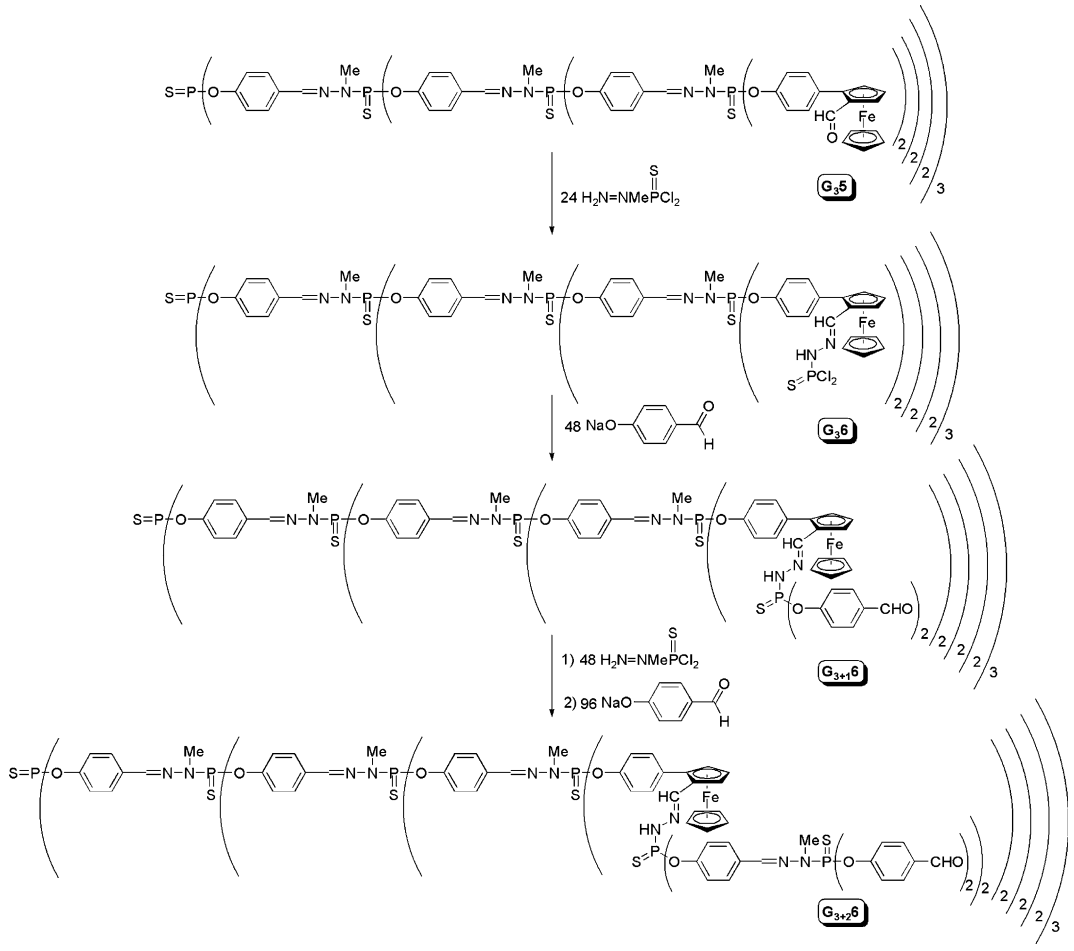

Scheme 2. Synthesis of Majoral's end-capped ferrocenyl dendrimers **5** and **6**.

spectroscopy. ^{31}P NMR spectroscopy was employed to ensure complete reaction of the 4-hydroxybenzaldehyde with the PCl_2 moieties and ^{1}H NMR spectroscopy was used to probe the subsequent aldehyde condensation reaction. Size exclusion chromatography was also used and the determined polydispersity (1.03–1.08) indicated that the dendrimers formed were essentially monodisperse. Matrix assisted laser desorption ionization time of flight (MALDI-TOF) mass spectrometry experiments were not possible due to reactivity of the hydrazone linkages.

Analysis of the electrochemical properties of the dendrimers show distinctive differences in the intensity of the redox waves and reversibility, depending on the layer in which the electroactive ferrocene is located. The dendrimers suitable for electrochemical study were the ferrocene-capped **5** dendrimers and for the various generations of **6,** systems incorporation the aryl aldehyde end group. For all dendrimers studied, a single oxidation/reduction wave is observed for the individual species showing that all the ferrocene units in a given dendrimer have the same redox potential and are electrochemically independent. In terms of the redox potentials, the difference between the dendrimers with terminal ferrocenyl groups and the "buried" ferrocene is due to the different functional groups on the ferrocene ring. For the terminal ferrocenes, $\mathbf{G_3}\mathbf{5}$ for example, an aldehyde is connected to the ring, while for the aryl aldehyde-capped dendrimers, a hydrazone is bound to the ferrocenes, as in $\mathbf{G_3}\mathbf{6}$. This results in a negative shift of the potential from ~0.81 to ~0.64 V for **5** and **6**, respectively. The addition of subsequent dendrimer layers has no significant effect on the potential. Two other observations were noted in comparison of the various dendrimers. The first is that the rate of electron transfer is greatly reduced upon confinement of the ferrocene within the dendrimer. In a related observation, it was also noted that the reversibility of the system is increased upon ferrocene confinement. In the case of ferrocene end-capped dendrimers **5**, deposition of a blue film on the electrode was noted and the reduction waves show a typical shape associated with stripping. However, with the ferrocene group protected within the dendrimer in **6**, these features were not observed showing that the encapsulation of the electroactive unit can add stability under electrochemical conditions. In terms of the chiroptical properties,

optical rotation measurements were obtained and almost no difference was noted based on the position of the ferrocene within the dendrimer. This indicates that the chemical environment about the chiral centers is not significantly perturbed by burying it within the dendrimer structure.

Togni and coworkers have reported the attachment of chiral ferrocenyl diphosphines to a dendritic skeleton. The "Josiphos" groups, as shown in Scheme 3 and Fig. 5, have been incorporated via a carbosilane linkage to a carbon of the cyclopentadienyl (Cp) ring of the ferrocene. The mononuclear Josiphos ligand system was proven to be an effective support for Rh-catalyzed asymmetric hydrogenation of alkenes [30]. Josiphos containing dendrimers have been constructed with arene (**9**), adamantyl (**10**) [31], and phosphazene (**11**, **12**) [32] cores and dendrimers containing up to 24 metallocene fragments [33] have been synthesized. The basic synthetic procedure is essentially identical for all the dendrimers. The Josiphos ferrocene **7** with a pendant amine functionality is reacted with an acid chloride, in the cases of the adamantyl and aryl cores, or is deprotonated with NaOMe and subsequently reacted with a P–Cl bond in the case of the phosphazene derivatives. The synthesis of a dendritic wedge containing two Josiphos moieties, compound **8**, is shown in Scheme 3 and the structures of the dendrimers **9**–**12** are given in Fig. 5. After generation of dendron **8**, the silyl ether protecting group is removed to produce a phenol, which is then coupled to the previously described cores via acid (HCl) elimination. All compounds have been characterized by exhaustive NMR methods as well as MALDI-TOF mass spectrometry. As expected, the NMR spectra are all indicative of a highly symmetrical system. For instance, the ^{31}P NMR spectrum of **11** exhibits only a singlet for the interior core P=N groups and the Josiphos portion appears as two doublets ($^4J_{P-P} = 40$ Hz) as the inequivalent phosphorous atoms couple in the periphery.

All Josiphos containing dendrimers **9**–**12** have been tested in the Rh-catalyzed asymmetric hydrogenation of dimethyl itaconate with excellent results. To generate the active catalytic species, the dendrimers were reacted with one equivalent (per Josiphos) of $[Rh(COD)_2]BF_4$ in CH_2Cl_2 for 15 min. All of the dendrimers tested were highly active, hydrogenation was complete in ca. 20 min, and the dendritic systems exhibited high ee values (>98%), regardless of the size, number of Josiphos groups or dendrimer generation. The monomeric model **7** showed similar activities and an ee of 99% for the identical reaction. This result demonstrates that incorporation of chirality in the dendrimer framework can be smoothly transferred to a substrate in a catalytic reaction and that each catalytic center is essentially sterically independent of its neighbours. For the larger dendrimers incorporating an adamantyl core, preliminary membrane filtration experiments show quantitative retention of the dendrimers [31] but results of hydrogenation in a continuous-flow reactor have not yet been reported.

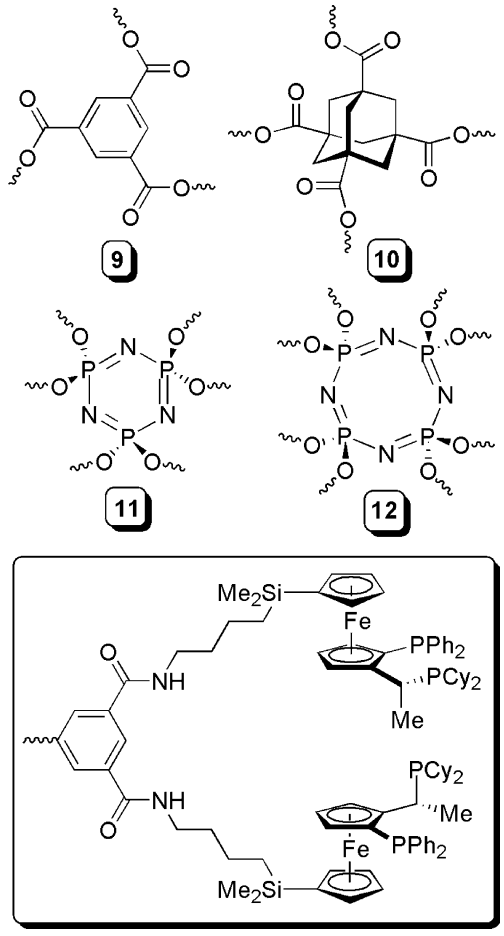

Fig. 5. Structure of Togni's Josiphos containing dendrimers **9**–**12**.

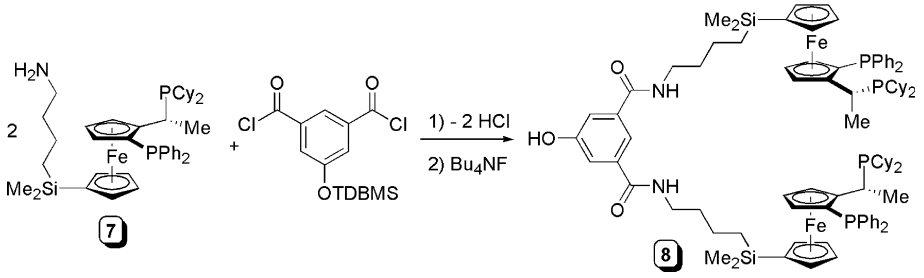

Scheme 3. Synthesis of Togni's Josiphos dendron **8**.

Most of the ferrocene containing dendrimers reported to date exhibit no electronic communication between the electroactive groups, as shown by the fact that oxidation or reduction takes place at a single, well-defined potential. However, the ability to connect the ferrocenes in a fashion that would allow communication could be of potential interest in adding flexibility to the redox receptivity of the dendrimers. Cuadrado et al. [34] reported the first example of unambiguous electronic coupling of ferrocenes in a carbosilane dendrimer framework. Recent work by Kaifer and coworkers [35] has shown that differentiation of the redox properties of ferrocene moieties within a dendrimer is possible in a chemically reversible fashion. Dendrimers containing ferrocenes with DAB type alkylamine backbones were synthesized. The reaction of (ferrocenylmethyl)trimethylammonium iodide **13** with the amine NH functions proceeds in the presence of K_2CO_3. The dendrimer **14**, shown in Scheme 4, was isolated in 20% yield; the heptasubstituted derivative, missing one ferrocene group, could also be obtained in 40% yield. The species were separated by column chromatography.

The key to modulation of the electronic communication is the quaternization of the bridging amine group (see Fig. 6), which can be achieved irreversibly with iodomethane or reversibly with protic acids, such as HCl. In the neutral, unprotonated state, some moderate electronic communication is observed between the ferrocene centers, presumably mediated by the lone pair of electrons of the amine nitrogen. Upon reaction with acid or iodomethane, the charged ammonium bridge effectively blocks any electronic interaction between the metal centers. As the redox potential of the charged and uncharged portions are significantly different ($E_{1/2}$ = 0.50 and 0.61 V for **14** and fully protonated **14**, respectively) it is possible to observe two distinct redox waves. Cyclic voltametry was performed on **14** during titration with 1 M HCl. On addition of 3.5 equivalents of acid,

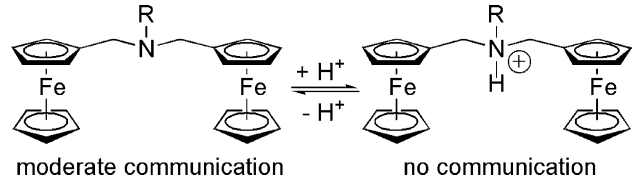

Fig. 6. Electronic communication in Kaifer's ferrocenyl dendrimer **14**.

the CV clearly exhibits two waves, due to the partial protonation of the dendrimer. Addition of 10 equivalents of acid results in full protonation and the observation of a single wave.

In somewhat related work, Salmon and Jutzi [36] have reported the synthesis of similar ferrocene-functionalized DAB dendrimers to Kaifer but with only one ferrocene unit per dendrimer arm. The first step of the reaction sequence consists of reaction of the ferrocenyl aldehyde with the DAB amine. The resulting imine is reduced with $NaBH_4$ to generate the desired dendrimers. A simplified diagram detailing the synthesis of the first generation dendrimer $\mathbf{G_1}$**15** is shown in Scheme 5. The synthesis has been carried out up to and including the fifth generation, which incorporates 64 ferrocene groups and 126 amine functionalities in the dendrimer backbone. All the dendrimers were prepared in good yields and are soluble in common organic solvents, such as CH_2Cl_2 and toluene. However, reaction of the dendrimer with anhydrous HCl gas, also shown in Scheme 5, generates the cationic ammonium dendrimers **16** and results in drastic changes to the solubility properties. The resultant protonation of the dendrimer backbone amines renders the dendrimers insoluble in the above solvents but allows for dissolution in polar solvents such as DMSO, ethanol and water. The third generation cationic dendrimer $\mathbf{G_3}$**16** is depicted in Fig. 7.

All of the protonated dendrimers exhibited fully reversible redox behavior in DMSO solvent. Only one signal is observed in the cyclic voltamograms, and thus

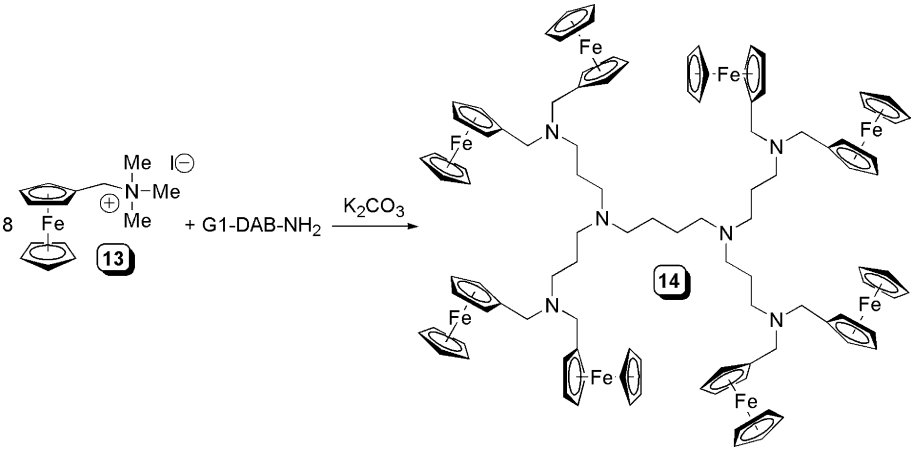

Scheme 4. Synthesis of Kaifer's ferrocenyl DAB dendrimer **14**.

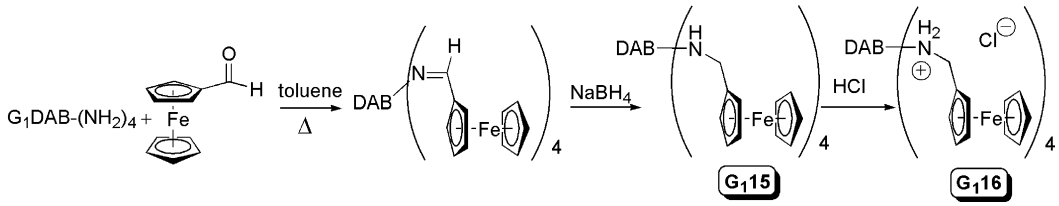

Scheme 5. Synthesis of Jutzi's water soluble ferrocenyl DAB dendrimers **16**.

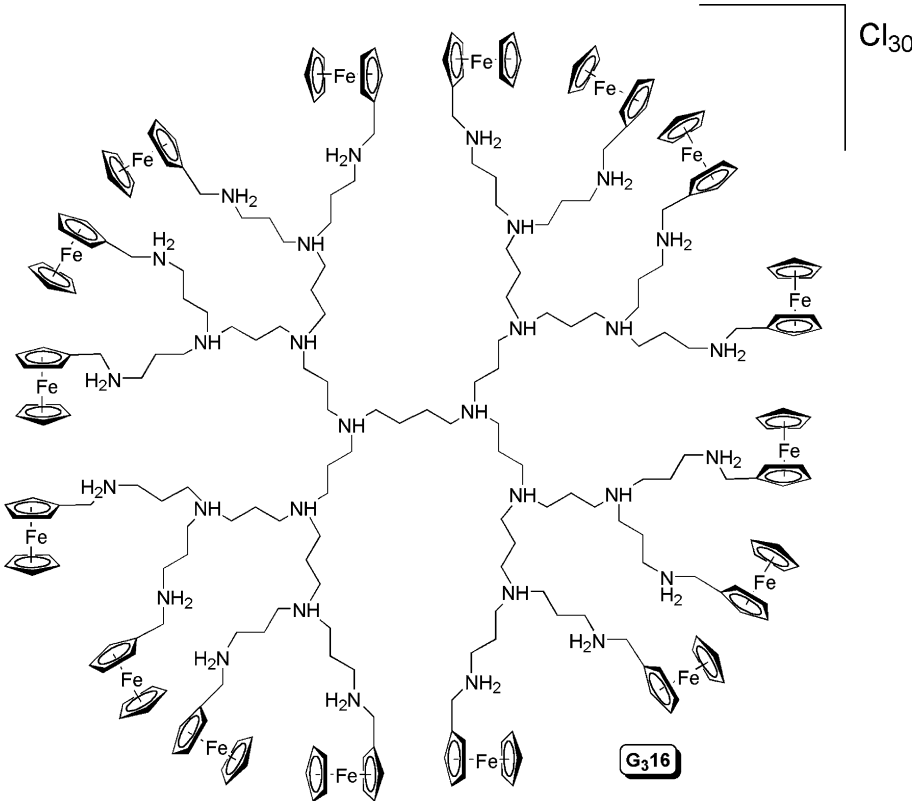

Fig. 7. Structure of Jutzi's water soluble ferrocenyl DAB dendrimer $\mathbf{G_3 16}$.

all the ferrocenes are electrochemically equivalent and independent. The ferrocenyl ammonium units in dendrimers of type **16** were more difficult to oxidize than parent ferrocene dendrimers **15** by 90 mV, due to the addition of a cationic group adjacent to the ferrocene ring. Also, as a result of increased solubility in polar solvents, adsorption of the oxidized species onto the electrode surfaces was not observed.

Ferrocenyl dendrimers incorporating liquid crystalline promoting functions have been recently reported by Deschenaux and coworkers [37]. Two species were reported and differ in the position of the ferrocene moiety in the dendritic structure and the nature of the liquid crystalline promotor. As shown in Fig. 8, dendrimer **17** has the ferrocenyl group between the dendrimer core and the cholesterol liquid crystalline portion. In compound **18**, the ferrocene is located in the extreme periphery of the dendrimer and the liquid crystalline segment consists of a rod of contiguous aromatic rings. Both the dendrimers exhibit liquid crystalline properties; evidence for the liquid crystalline nature of the dendrimers was established by differential scanning calorimetry and polarized optical microscopy and the nature of the mesophases was probed via X-ray diffraction studies. The isotropization temperatures were somewhat lower for **17** (169 °C) than for **18** (256 °C), likely due to the differing nature of the liquid crystalline promoting groups. While this initial study does not allow for the strict evaluation of structure/property relationships, it does indicate that the liquid crystallinity of the dendrimers is not dependent on the position of the ferrocene moiety. This allows for potential flexibility in the construction of future dendrimers as the position of the organometallic can be varied without significantly affecting liquid crystalline properties.

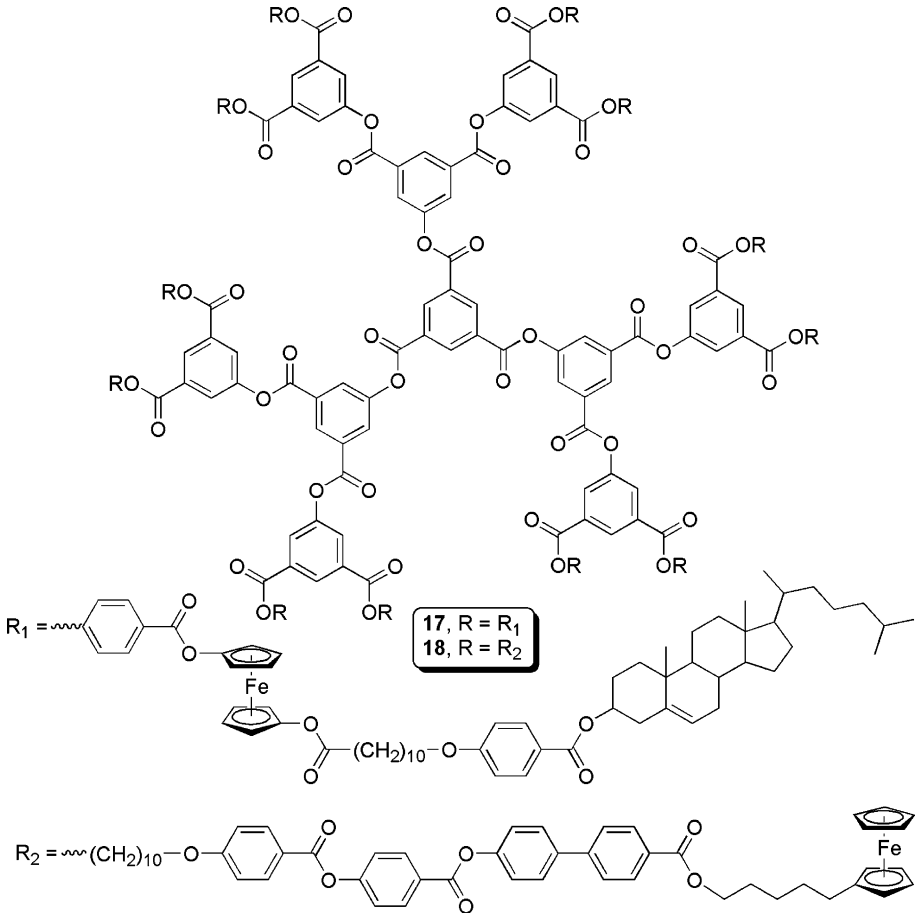

Fig. 8. Structures of Deschenaux's liquid crystalline ferrocenyl dendrimers **17** and **18**.

A mixed cobaltocene–ferrocene dendrimer was recently synthesized by Cuadrado and coworkers [38] utilizing various DAB-amine backbones. These dendrimers combine the stable, reversible electrochemical properties of ferrocene (oxidation) with similar characteristics of cobaltocenium (reduction). Combining these redox systems in the same dendrimer should lead to interesting properties. The heterogeneously peripherally substituted dendrimers were synthesized simply via addition of an equimolar ratio of the acetyl chlorides of ferrocene or cobaltocenium hexafluorophosphate to the DAB amine dendrimers. The zeroth through the third generation dendrimers **19** were synthesized; the third generation containing 32 substituted end groups. A model compound **20** containing one ferrocene and one cobaltocenium cation separated by a 1,4-diamido butane linkage was also synthesized to aid in characterization. Ideally, the dendrimers should contain equivalent amounts of the ferrocene and cobaltocenium randomly distributed over the periphery. However, this in not the case as treatment of reaction mixtures with CH_2Cl_2 and MeCN resulted in isolation of fractions containing different ratios of organometallic groups, perhaps not surprising based on the synthetic method employed. The structures of the dinuclear model **20** as well as that of the idealized, i.e., equimolar quantities of ferrocene and cobaltocenium, second generation dendrimer $\mathbf{G_2}$**19** are shown in Fig. 9.

The solubility of the dendrimers can also be controlled by variation of the stoichiometry of the ferrocene and cobaltocenium starting materials. By increasing the amount of charged cobaltocenium, the subsequent dendrimer's solubility in water is increased. Conversely, by loading the structure with neutral ferrocene, water solubility is decreased but the dendrimer has enhanced solubility in CH_2Cl_2. This easy tuneability of the surface charge density, and thus solubility properties, is one of the potentially useful properties of this dendrimer system.

The dendrimers were characterized by NMR spectroscopy, electrospray ionization mass spectrometry (ESI-MS) and total X-ray fluorescence (TXRF). The ^1H and ^{13}C NMR spectral signals for the ferrocene and cobaltocenium moieties were essentially identical to those of the dendrimers containing only the individual metallocenes and integration of the ^1H NMR signals was used to determine the ratio of the peripheral metallocenes in the dendrimers. TXRF analysis was used to

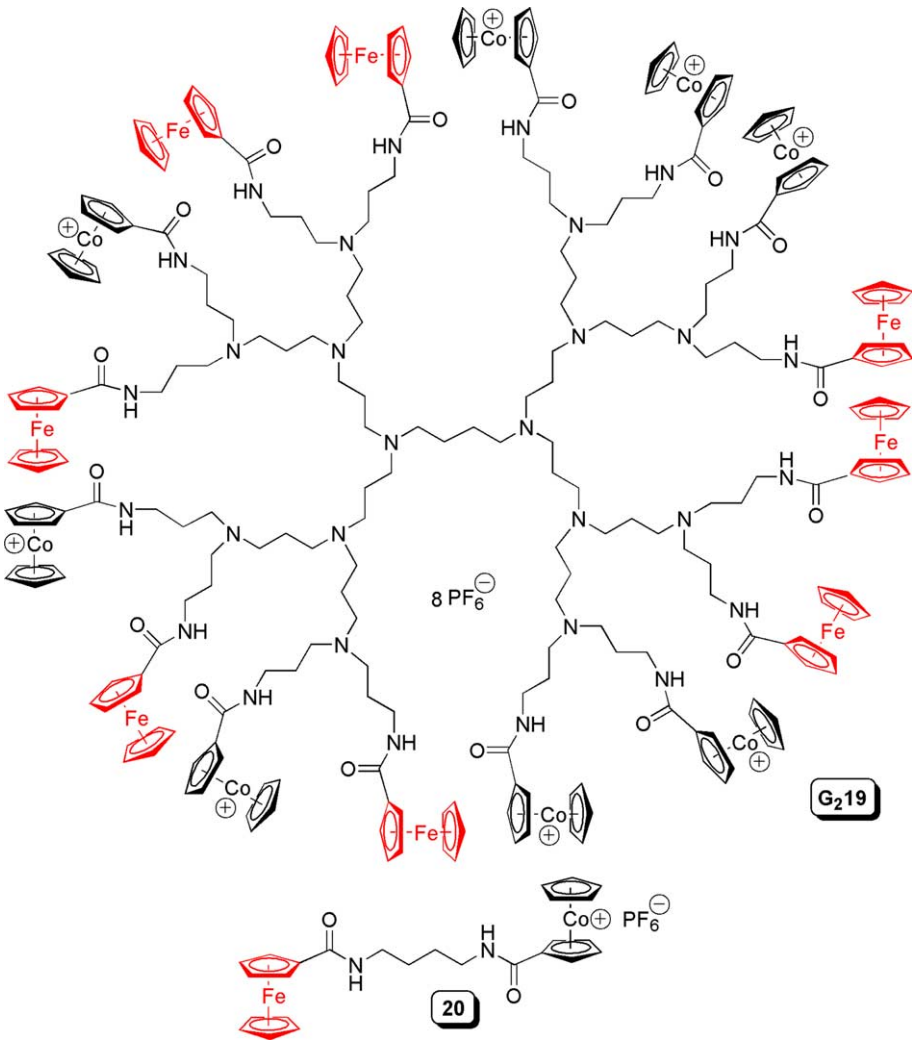

Fig. 9. Structures of Cuadrado's mixed ferrocene cobaltocene dendrimer **$G_2$19** and model species **20**.

confirm the ratios determined from NMR experiments and cobaltocenium: ferrocene ratios in the bulk mixture were 3:1 for the zeroth generation dendrimer **$G_0$19**, 6.5:1.5 for **$G_1$19**, 13:3 for **$G_2$19** and 19:13 for **$G_3$19**. The ESI-MS experiment confirmed the presence of multiply charged species, due to sequential loss of counteranions.

The cyclic voltamograms of dendrimers **19** and the divalent model **20** were also investigated. All the dendrimers exhibit two waves; one oxidation at approximately 0.60 V, assigned to the $Fe^{II/III}$ couple for multiple, non-interacting ferrocenes and a single reduction peak at about −0.70 V, due to the $Co^{II/I}$ couple for the cobaltocenium cations, again which are presumably non-interacting. There is also some evidence of deposition of the dendrimers on the electrode during reduction due to the change of charge during the electrochemical process. The reduced neutral dendrimer precipitates on the electrode and subsequently redissolves during the return oxidation process. Also, the ferrocene/cobaltocenium ratio calculated from cyclic voltametry is in good agreement with the NMR and TXRF results.

Films of the second generation mixed metallocene dendrimer **$G_2$19** have been coated on electrode surfaces and show a remarkable degree of stability and reversibility under the conditions of the CV experiment. The electrodes were subjected to over 100 scans with no loss of current response or drift of redox potential for either the ferrocene or cobaltocenium centers. These dendrimer-modified electrodes were further derivatized by immobilization of glucose oxidase on the surface as well. For biochemical processes, the combination of the ferrocene and the cobaltocenium fragments forges a well-matched pair as the iron centers can act as mediators for anaerobic enzymatic processes while the cobaltocenes can participate in reactions under aerobic conditions. Glucose was detected using the oxidase/dendrimers-modified electrode via amperometric response by either monitoring the enzyme-mediated

oxidation of ferrocene or, conversely, by measurement of the reduction of dissolved oxygen by the cobaltocenium cations. The intense currents observed were not apparent with an electrode modified with the oxidase only and thus the bimetallic dendrimer plays a critical role in the sensitivity of the constructed electrode.

A novel dendritic structure has been reported in which the core of the dendrimer consists of a cyclotriphosphazene moiety [39]. While most dendrimer cores allow for introduction of three or four dendrimer arms, aryl or adamantyl for example, incorporation of the phosphazene core allows for facile incorporation of six separate dendrons about the core. Majoral and Togni originally reported the use of the P_3N_3 core in the construction of organic dendrimers [40] and in the generation of Josiphos containing dendrimer **11**, respectively. As well, the phosphazene function is chemically and thermally inert under a wide variety of conditions. The synthesis involved generation of a diferrocenyl phenol and subsequent addition to hexachlorotriphosphazene, $Cl_6P_3N_3$, employing NaH as a base. An excess of the dendron was used (10 equivalents) but some uncoupled products arising from incomplete substitution are present. The structure of the dendrimer **21** is depicted in Fig. 10. With the chosen dendron, steric crowding appears to be an issue. The completely functionalized dendrimer **21** was isolated in 26% yield after preparative thin layer chromatography and characterized by multinuclear NMR and IR spectroscopy as well as MALDI-TOF mass spectrometry.

Electrochemical studies on **21** indicate that all 12 of the ferrocene groups are electrochemically equivalent. A single reversible wave with an $E_{1/2} = 0.41$ mV (vs. SCE) in CH_2Cl_2 is observed. Some anodic stripping was noted as the current of the cathodic wave was slightly larger than that of the anodic wave, indicating potential deposition of the oxidized product on the cathode surface.

A number of related ferrocene-substituted triphosphazenes, including a hexaferrocene **22**, have also been synthesized [41]. An example is also shown in Fig. 10. These species do show similar electrochemical behavior in that a single, reversible wave is observed, indicating that all the ferrocene units are uncoupled and react independently. While not technically dendrimeric, compound **22** provides a further example in which the triphosphazene core is used as a hexa-substituted support for multiple redox active centers.

2.2. Dendrimers containing non-ferrocene organometallic groups in the periphery

These types of dendrimers constitute an important class of compounds and have been employed in a variety of fields. Very often, these are the species at the forefront of prototypical species that are attempting to "bridge the gap" between homogeneous and heterogeneous catalysis. The goal of this area is to combine the most favourable properties of each of the two types of catalysis. Ideally, the accessibility and precise, synthetically variable control of the structure of the catalytically active site, features available to homogenous, monomeric systems, would be coupled with facile catalyst separation from product streams or potential isolation of reactive sites, hallmarks of heterogeneous catalysis. In addition, the effects of functional group concentration on dendrimer peripheries, probed elegantly with the previously described ferrocene chemistry, can be utilized to alter reactivity compared to non-dendrimer systems and to investigate modes of catalyst decomposition.

One of the first reported successes in the dendrimer field as a whole was the attachment of monoanionic, ter-

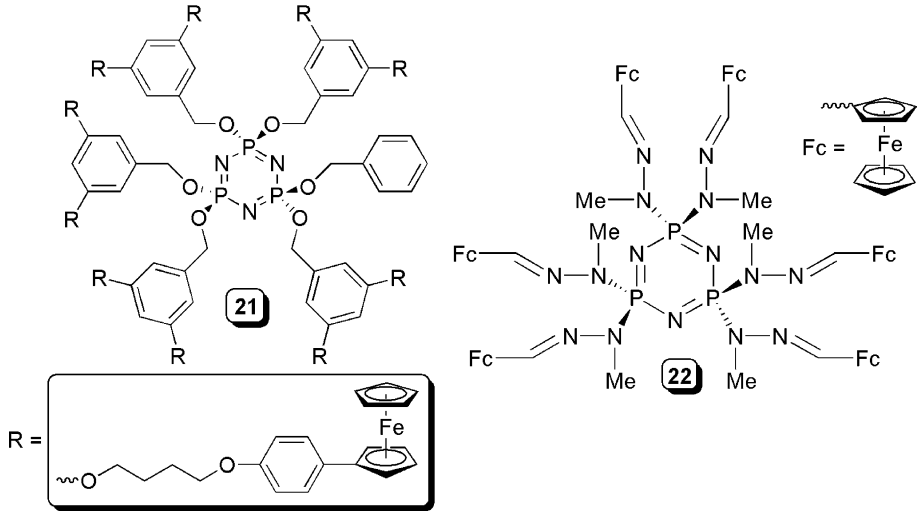

Fig. 10. Structures of Sengupta's ferrocenyl triphosphazene dendrimer **21** and related species **22**.

dentate chelating "NCN" type pincer nickel moieties in the periphery of a carbosilane dendrimer. As described in the introduction, dendrimers **$G_0$2** and **$G_1$2** were successfully employed in the Kharasch addition, with comparable activity to monomeric species. Based on these preliminary experiments, some modifications to the pincer containing dendrimers were investigated to further elucidate the factors that affect catalyst performance and to determine if these systems were amenable to membrane filtration techniques [42,43]. One of the first details addressed was the nature of the linking group between the dendrimer and the organometallic pincer species. In the original report, a carbamate moiety was installed in **2**, which allowed for rapid and simple installation of the pincer on the dendrimer skeleton. However, this linker could potentially limit further reactivity, for example, with alkyl lithium reagents. To help overcome these potential deficiencies, a dendrimer was constructed in which the link between the aryl ring of the pincer and the dendrimer was changed to a silyl group. Based on this methodology, a small library of dendrimers was assembled and the effect of peripheral crowding and the proximity of reactive metal centers could be systematically probed.

The synthesis of the new pincer containing dendrimers consisted of a four step reaction sequence shown in Scheme 6; (1) hydrosilation of an appropriately substituted allyl-terminated dendrimer with $HSiMe_2Cl$, (2) metathesis of the Si–Cl bond with excess 3-Li-1,5-$(CH_2NMe_2)_2C_6H_3$ (**23**) to install the pincer moiety on the dendrimer, (3) selective lithiation between the pincer arms with *t*BuLi, (4) transmetallation of the lithiated dendrimer with $NiCl_2(PEt_3)_2$ to give the desired NCNNi dendrimers.

Variation in the dendrimers was introduced via differing substitution patterns in the branching points, the structures of the NCNNi dendrimers **24**–**26** are shown in Fig. 11. For example, the first generation dendrimer **$G_1$24** contains three pincer moieties per silicon branching point in the periphery, giving a dendrimer with ideally 12 Ni containing pincer functions. The related G_1 dendrimer **26** has only two pincer moieties per arm and the additional valency of the silicon is accommodated by a methyl group. In addition, an "extended" system incorporating an additional $–CH_2CH_2SiMe_2–$ fragment between the dendrimer and the pincer (**25**) was synthesized. This was accomplished by employing one extra sequence of allylation and hydrosilylation prior to introduction of the pincer moiety. All the pincer containing dendrimers were characterized by multinuclear NMR spectroscopy as well as mass spectrometry and elemental analysis.

While the synthetic route was simple and effective, there were some problems associated with the final reaction step. The presence of lithiated pincer moieties is synthetically very useful for the introduction of various metal centers but also extremely sensitive to traces of water. Analysis of the spectroscopic and elemental analysis data showed that the nickellation of the pincer moiety was incomplete, in general only 80–90% of the pincer sites were metallated. This is proposed to be due to partial hydrolysis of the reactive polylithiated species

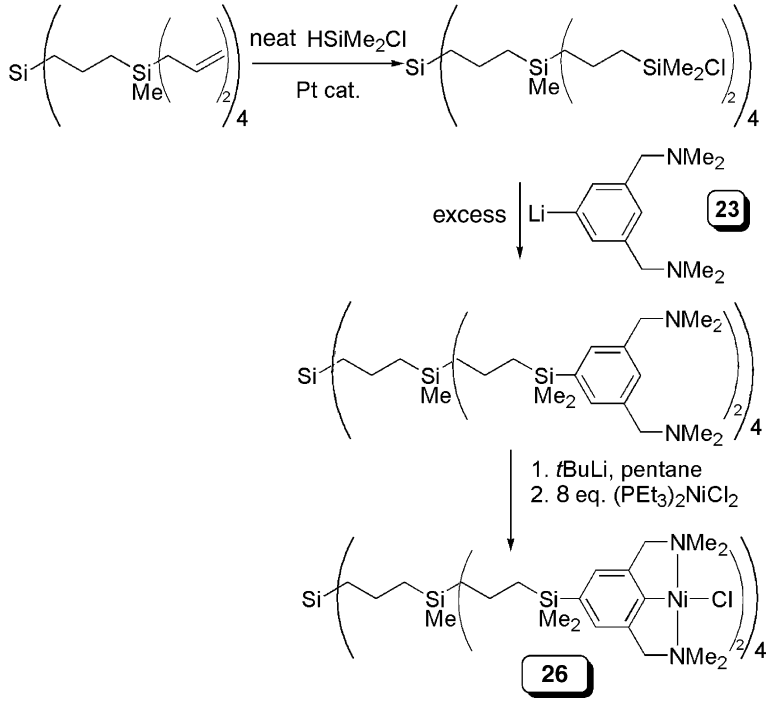

Scheme 6. Reaction pathway for generation of van Koten's carbosilane NCNNi dendrimer **26**.

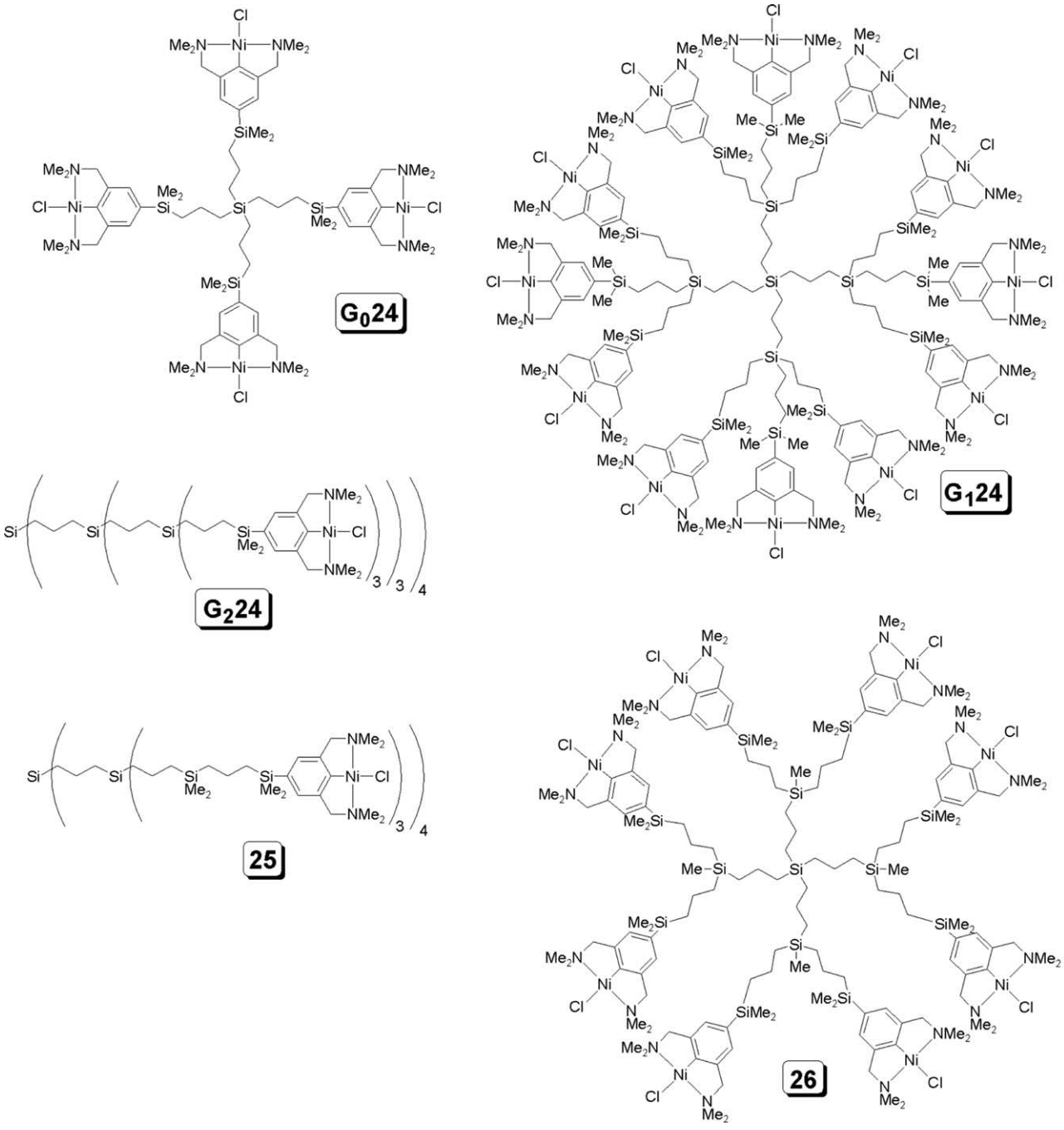

Fig. 11. Structures of van Koten's carbosilane NCNNi dendrimers **24**–**26**.

during the nickellation reaction. Separate experiments show that greater than 98% lithiation is achieved with non-nickellated dendrimers of type **24**, based on quenching studies [44,45], so adventitious introduction of moisture is likely the source of the observed partial metallation and not due to incomplete lithiation of the pincer groups. The presence of non-metallated sites was evident in the NMR spectra of the products. The degree of metallation observed in the ^{1}H NMR spectra, based on integration, matches results from elemental analysis. Mass spectrometry also showed the presence of these defects in the dendrimer structure.

The redox chemistry of the nickellated dendrimers was investigated. As the redox processes involves *both* an electrochemical and a chemical step, simple Nernstian behaviour is not observed. For NCNNi^{II}Cl pincer complexes, oxidation of the nickel center to Ni^{III} is followed by addition of chloride to generate NCNNi^{III}Cl$_2$ (**27**, see Scheme 7) in the presence of a chloride source, in this case from the supporting electrolyte, Bu_4NCl.

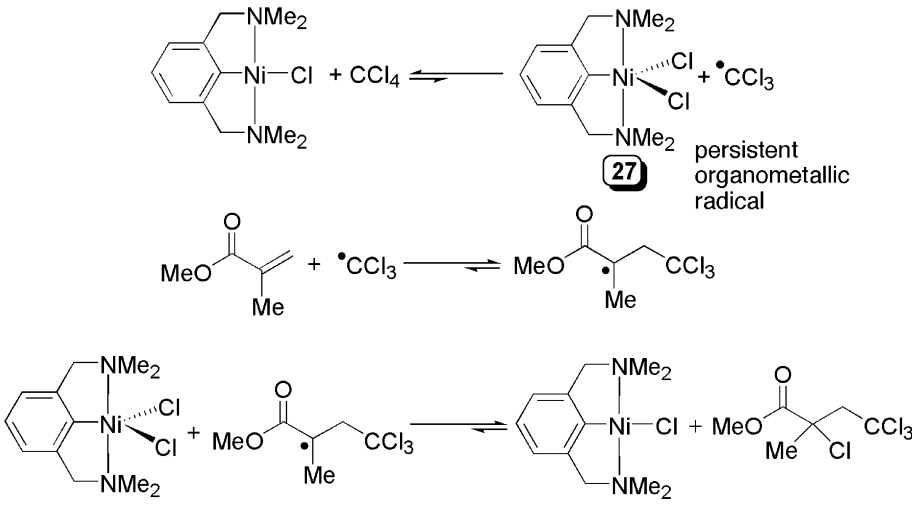

Scheme 7. Reaction mechanism of Kharasch addition catalyzed by NCNNi pincers.

For the dendrimer systems, only a single oxidation and reduction wave is observed for the individual species; all the Ni centers are electrochemically equivalent and independent. The calculated $E_{1/2}$ values (taken as the average of E_{ox} and E_{red}) were essentially equivalent (−0.32 to −0.35 V) irrespective of dendrimer.

The main contribution from this work was the detailed analysis of the effect of the density of peripheral functional groups on the catalytic activity of the dendrimers in the Kharasch addition. The Kharasch addition is an atom transfer radical addition reaction between an olefin and a polyhalogenated alkane; a simple mechanism of this reaction, catalyzed by NCNNi pincers, is shown in Scheme 7. The model reaction studied was the selective, stoichiometric Kharasch addition of CCl_4 to methyl methacrylate. Under conditions of excess methyl methacrylate, however, with catalytic quantities of NCNNiCl and CCl_4, low polydispersity poly(methyl methacrylate) can be generated. Based on dendrimer, the activity of the NCNNi moieties showed a remarkable degree of variation. The zeroth generation dendrimer **$G_0$24** exhibited very similar activity to that of monomeric analogues, whereas the second generation dendrimer **$G_2$24** was essentially inactive. There was obviously a strong correlation between the dendrimer generation and catalytic activity in the Kharasch reaction. This negative dendrimer effect was ascribed to the proximity of the surface Ni pincer functions and was clearly evident in comparison of the reactivity of the various first generation dendrimers. The highly branched, high nickel content, compact dendrimer **$G_1$24** exhibits activity, in terms of initial turnover frequency per Ni center, approximately half that of the zeroth generation. In addition, the reaction profile is indicative of significant catalyst deactivation, after 60 min there is essentially no additional conversion. However, extension of the length of the dendrimer arms in **25**, or dilution of the nickel content on the dendrimer surface in **26**, results in a significant boost in catalyst stability. While **$G_1$24** is essentially inactive after 60 min and 20% conversion, both **25** and **26** do not show signs of catalyst degradation and full conversion is achieved in 22 h.

Analysis of the kinetic behaviour of the reaction and fate of the catalytic NCNNi species allowed for postulation of possible deactivation mechanisms of the catalysts in the dendrimer framework. For all the species, a purple precipitate could be isolated from the reaction mixture. In the case of the catalytically active dendrimers, the formation of this precipitate was only evident near the end of the reaction, under conditions of low olefin concentration. In the case of the deactivated compounds, this purple precipitate was noted early in the reaction and coincides with the observed reduction in reaction rate. Independent synthesis and comparison of EPR spectra show this product to be a stable, persistent $NCNNi^{III}Cl_2$ radical like **27**.

From this data, a plausible mechanism for catalyst deactivation can be formulated. As shown in Scheme 7, the initial step of the catalytic reaction is the generation of a $NCNNi^{III}Cl_2$ complex in conjunction with a $Cl_3C^{\cdot}$ radical. Salient to the regeneration of the active Ni^{II} catalyst is halide abstraction from the Ni^{III} center by the radical product precursor P$^{\cdot}$. However, if the generated $Cl_3C^{\cdot}$ radical were to undergo a termination process, such as radical coupling with an additional $Cl_3C^{\cdot}$, the Ni(III) species becomes trapped in this state and the active Ni(II) center cannot be regenerated. In this way, the high concentration of Ni centers on the dendrimer surface is detrimental to catalytic activity. During the initial radical formation step, a high local concentration of radicals is generated. This increases the chance for irreversible coupling of two $Cl_3C^{\cdot}$ molecules and concurrent removal of catalytically active Ni centers.

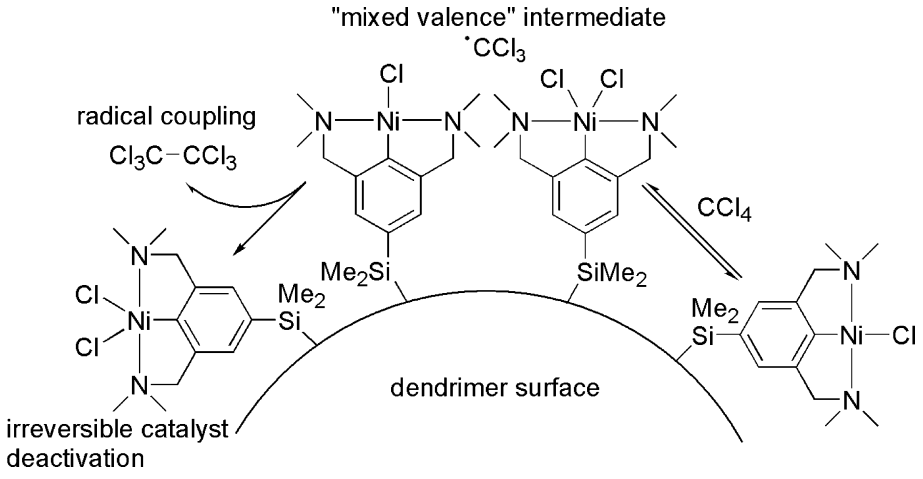

Fig. 12. Proposed deactivation pathway of NCNNi containing dendrimers in Kharasch addition.

By dilution of the Ni concentration on the dendrimer surface or by extension of the inter nickel distances, this effectively dilutes the local radical concentrations and therefore reduces the rate of catalyst deactivation. It is this *irreversible* formation of catalytically inactive Ni(III) centers that ultimately is the cause of the reduced reactivity. A depiction of a possible deactivation process is given in Fig. 12.

The pincer-based carbosilane dendrimers **$G_0$24** and **$G_1$24** were tested for their degree of retention under membrane filtration conditions. Using a SelRO-MPF-50 membrane, the retention of **$G_0$24** and **$G_1$24** were 97.4% and 99.75%, respectively. As expected, the larger dendrimer is retained to a greater degree and the degree of retention was sufficient to perform test catalysis. For both **$G_0$24** and **$G_1$24** under batch conditions, the precipitation of the purple decomposition product was noted after 40 min. However, for the first generation dendrimer **$G_1$24**, the decomposition product still showed activity in the Kharasch addition. Addition of Bu_4NBr prevented formation of the decomposition product but resulted in somewhat lower initial reaction rates and incorporation of Br into the product, due to halide exchange with the catalyst. Continuous flow membrane reactions were also attempted with **$G_1$24**. While no precipitation of decomposition products was noted, there was significant loss of catalytic activity after 33 h. Tests of the retained and filtered fractions indicated that the catalyst was retained by the membrane (98.6%) but showed no activity. It was proposed that the reactive radical intermediates might be interacting with the functional groups of the membrane material and thus influencing the observed reactivity. While the catalyst was effectively retained, new membranes are needed that are compatible with the reaction conditions to successfully construct a usable system for continuous operation.

Subsequent dendrimer chemistry utilizing the pincer systems involving gas-sensing applications has also been developed. The synthesis of these dendrimers employed a rapid esterification reaction between 4-hydroxy-NCNPt groups with acetyl chlorides which were coupled to a benzene core [46]. The synthesis of these species was performed via a convergent route. Zeroth and first generation dendrimers **28**, shown in Fig. 13, were prepared via this route and were fully characterized by multinuclear NMR and UV–Vis spectroscopies as well as mass spectrometry. These dendrimers were successfully employed as sensors for SO_2, a known property of NCNPt pincer species [47,48]. In addition to the characteristic colour change from colourless to orange upon exposure of the Pt pincer to an atmosphere of SO_2, there is a distinct change in solubility of the SO_2 adduct. While the uncomplexed dendrimers are relatively insoluble in THF, the adducts fully dissolve. The SO_2 binding strength and associated spectroscopic factors were not affected by incorporation into the dendrimer framework.

Based on previous studies, NCNPt pincers are also effective sensors for SO_2 in the solid state [48]. To exploit this characteristic, a solid state sensor was fashioned using a quartz crystal microbalance by grafting a variety of NCNPt molecules onto the microbalance disk [49]. The microbalance can detect the minute changes in net mass of the dendrimers-modified sensor disk due to complexation or removal of SO_2. Tests with monomeric 4-hydroxyNCNPt showed promising results in terms of gas detection but the sensor system was not stable as the NCNPt slowly sublimed at operating temperatures (50 °C). By using higher molecular weight dendritic structures, such as **29** shown in Fig. 14, this problem was circumvented and a stable sensor may be constructed. Sensors constructed from **28** or **29** could reliably and reversibly detect concentrations of SO_2 at 5 and 10 ppm, respectively. The high-end detection limit for both species was approximately 800 ppm. Moreover, the response to changes in SO_2 concentration in the gas stream was virtually instantaneous, an advantageous attribute for a potential device. Also,

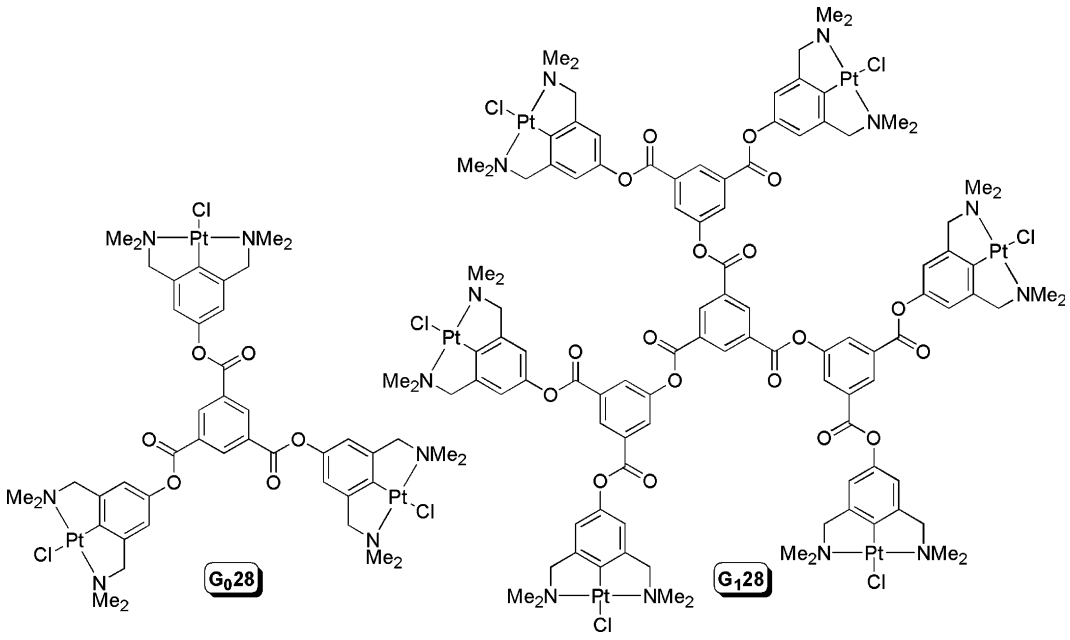

Fig. 13. Structures of van Koten's NCNPt pincer containing dendrimers **28** for solution SO_2 gas detection.

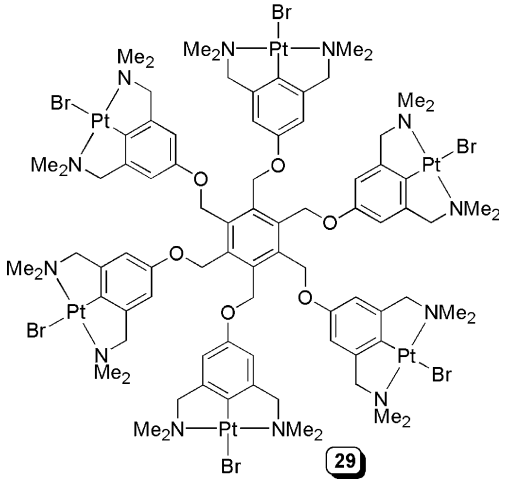

Fig. 14. Structure of van Koten's NCNPt containing dendrimer **29** for use in a solid state SO_2 detector.

there is no need to purge the system after gas detection as the sensor responds continuously to variation in gas concentration, preventing the need to purge the system between analyses. Finally, addition of impurities to the system, such as organic solvents (benzene, toluene, aniline, methanol, nitromethane) or other gases (NH_3, CO, CO_2, H_2O) does not effect the sensitivity or response of the system.

The pincer moiety has also been introduced into a variety of dendritic structures via non-covalent bonding modes. Dative metal–heteroatom bonding interactions have been employed by Reinhoudt to generate polymeric and well-defined dendritic structures with SCS pincer Pd units coupled with nitriles [50]. Incorporation of phosphorus donors (PCP-type pincer ligands) allowed for the synthesis of heterometallic dendrimers with Ni, Pd and Pt centers [51]. The NCN pincer function has also been incorporated in a dendrimer molecule. Electrostatic interactions, in a similar fashion to the H-bonded dendrimers of Astruc (see Section 2.1), are the key to incorporation of the NCN pincer organometallic fragment into the dendritic framework [52]. Utilizing NCNPd species in which a sulphate group is terminally incorporated into an alkyl chain on the *para* position of the pincer aryl ring, up to eight pincer moieties have been introduced into a dendrimer containing an octacationic ammonium core and a variety of polar or apolar dendritic arms. The cationic Pd species **31** could be generated via two separate routes. Reaction of the Pd–Cl dendrimer **30** with eight equivalents of $AgBF_4$ generated **31**. The structures of the dendrimers **30** and **31** are shown in Scheme 8 and have been characterized by multinuclear NMR spectroscopic studies, including DOSY experiments, and by ESI mass spectrometry [53]. Although halide scrambling is observed, the MS data clearly indicate that an octamer was formed and was stable in solution.

The NCNPd dendrimers **30** and **31** have been tested as Lewis acid catalysts in the aldol condensation of benzaldehyde and methyl isocyanatoacetate. Test reactions showed that incorporation of the active Pd catalyst into the dendrimer framework does not hinder catalytic activity and the dendrimer is highly active. Indeed, the % conversion, turnover frequency and the *cis*/*trans* ratio of the products were essentially identical for a monomeric model complex and the dendrimer. This methodology could potentially allow for facile variation and

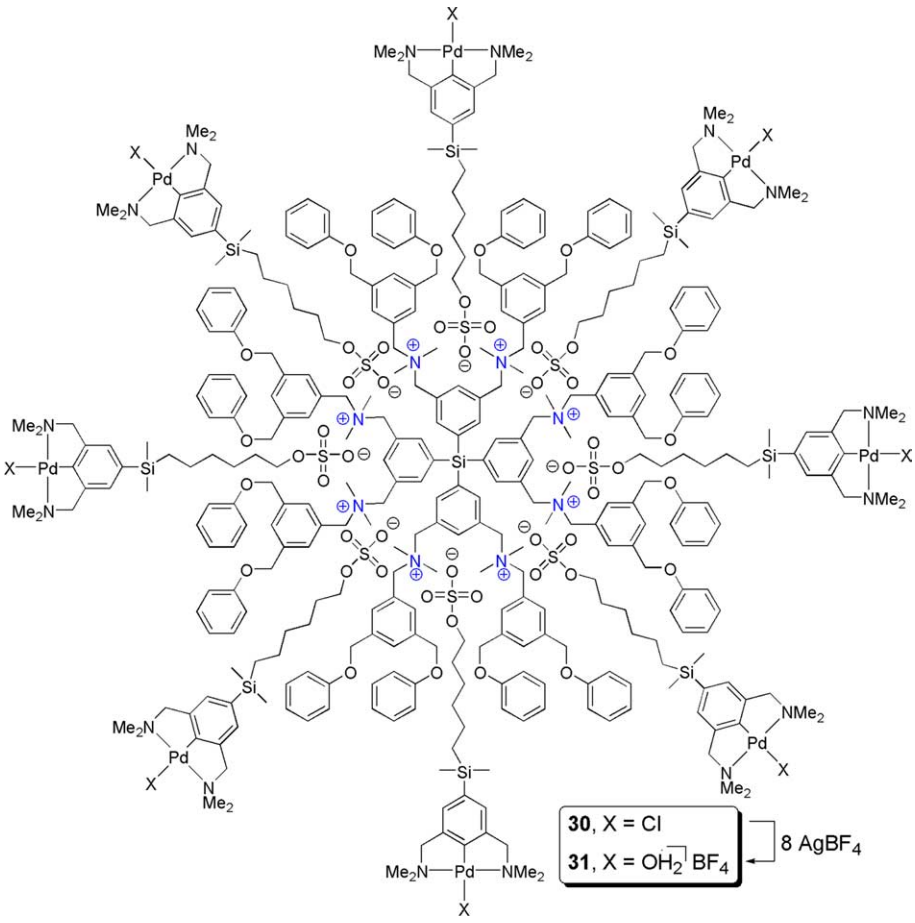

Scheme 8. Synthesis of van Koten's non-covalent assembled dendrimers **30** and **31**.

introduction of organometallic or other functional groups into a dendrimer framework.

Hurley and Mohler [54] have reported the synthesis of a DAB-amine-functionalized dendrimer with $CpW(CO)_3Me$ moieties. These species were studied as carriers for groups active in the scission of double-stranded DNA. The synthesis of these species was affected by a condensation reaction of the appropriate DAB amine with the activated succinimide ester of the organometallic fragment. An example of the first generation dendrimer $\mathbf{G_1}$**32** is given in Scheme 9. Dendrimers of type **32** were constructed out to the third generation along with a related spermine analogue (**33**). All syntheses were effected in good yields (58–70%).

The rationale for using the dendritic scaffold was fourfold. Studies involving DNA cleavage showed that two radical centers are needed to react sequentially to effectively cleave double-stranded DNA. As such, incorporation of the active fragments into a dendrimer will allow for close proximity of the reactive groups and potential cooperative effects. Secondly, the amine functionalities in the DAB backbone will be protonated at physiological pH, shown previously with Jutzi's ferrocenyl DAB dendrimers **15** and **16**, allowing for increased

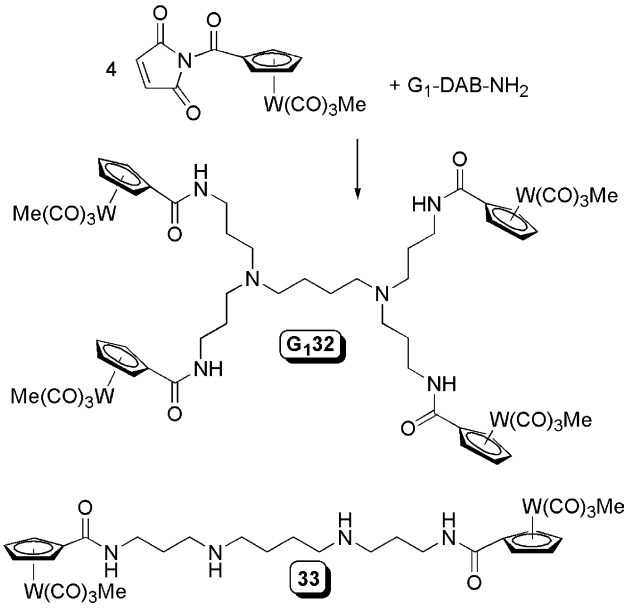

Scheme 9. Synthesis of Mohler's tungsten containing DAB dendrimers **32** and spermine analogue **33**.

water solubility, necessary for effective reaction rates and potential drug delivery. In addition, the positively charged ammonium centers will be electrostatically attracted to the anionic sugar–phosphate backbone of the DNA, which will increase the interaction between the dendrimer and DNA strands. Finally, the DAB dendrimers, in a variety of generations, are commercially available allowing for rapid screening of potentially active candidates.

The DNA cleavage studies were performed using all the above dendrimers with a standard DNA source, pBR322 DNA. While monomeric $CpW(CO)_3Me$ is an active cleaver of single-stranded DNA under photolysis conditions, it is completely inactive toward scission of double-stranded DNA. By incorporation of the active sites into the first generation DAB dendrimer, the activity of the tungsten centers in $\mathbf{G_1}\mathbf{32}$ increased nine-fold towards single strand cleavage. Also, $\mathbf{G_1}\mathbf{32}$ showed effective double strand cleavage indicating that there is a positive dendritic effect as the dendrimer structure was effectively able to deliver multiple radical species rapidly to the DNA strand. Unfortunately, the activity of the higher generation dendrimers could not be determined as they formed insoluble DNA/dendrimer aggregates, even under low pH conditions (<2).

Hoveyda and coworkers [55] have described the use of a carbosilane dendrimer for the recovery of Ru-based alkylidine olefin metathesis catalysts. Undoubtedly, olefin metathesis [56], with either ruthenium [57] or molybdenum [58] catalyst systems, is one of the more important reactions in polymer chemistry and natural product synthesis [59] and the ability to recover and reuse the catalysts would greatly impact the cost efficiency of these reactions. A simple dendrimer containing four active Ru sites was reported. To begin, a carbosilane dendrimer was synthesized with terminal styrenyl alkoxide moieties. This was reacted with 4.3 equivalents of the commercially available $Cl_2Ru{=}Ph(H)(PCy_3)_2$ (first generation Grubbs catalyst) and CuCl to generate dendrimer **34**, shown in Fig. 15. The related dendrimer **35**, differing only in that one PCy_3 has been replaced by an *N*-mesityl-functionalized imidazole, was generated in precisely the same fashion using second generation Grubbs catalyst. The yields of the air-stable dendrimers were 87% and 55% for **34** and **35**, respectively, for the final reaction step.

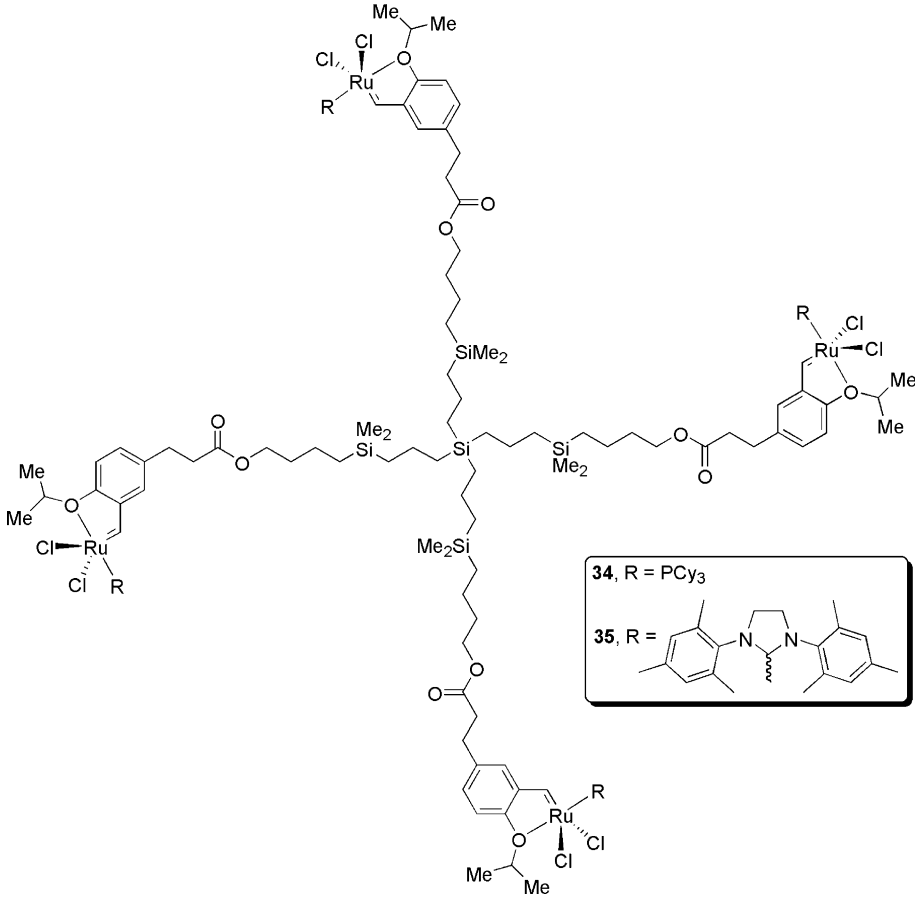

Fig. 15. Structure of Hoyveda's dendritic Ru olefin metathesis catalysts **34** and **35**.

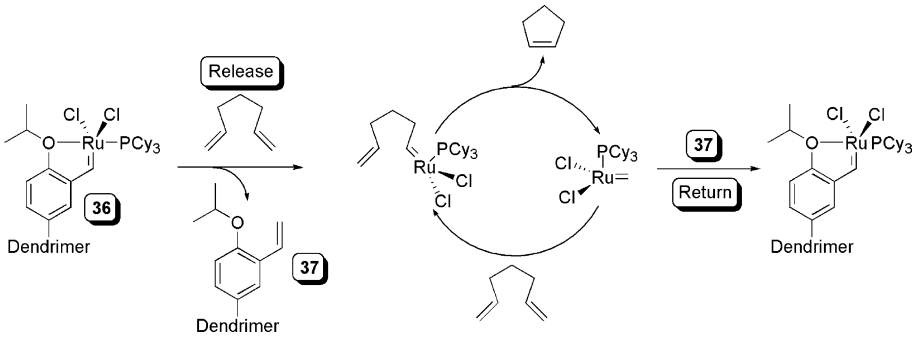

Scheme 10. Release/return mechanism for Hoyveda's Ru olefin metathesis catalysts.

The styrenyl alkoxide Ru metathesis catalysts operate via a unique mechanism, shown in Scheme 10, in which initial reaction of the Ru pre-catalyst **36** with olefins generates the proposed active catalytic species with expulsion of a styrene ether molecule. The styrenyl ether is relatively unreactive compared to most other olefins and does not participate to a large degree in the subsequent metathesis reactions. However, on consumption of the olefinic starting materials, the active Ru-carbene recombines with the styrene ether to regenerate **36**. This process, coined the release/return mechanism, has been employed to support a related metathesis catalysts within a polymer support [60]. There were noted, however, some problems with recovery of the Ru and with the activity of the polymer in subsequent reaction cycles, possibly due to folding of the polymer limiting access of the reactive groups. Thus, the well-defined structural characteristics of a dendrimer could potentially be employed to increase both the reaction rate and the degree of catalyst recovery. However, the release/return mechanism does have some fundamental problems associated with use in continuous flow or membrane filtration experiments. As the active catalyst is not bound to the dendrimer, metal species of small dimensions are free in solution and thus catalyst leaching would occur. Also, catalyst self-decay can occur which will also compete with the return step [55]. As such, these species are more suitable for recovery and reuse in batch reactions.

The Ru containing dendrimers were tested as catalysts in a number of metathesis reactions, including ring closing, ring opening, cross metathesis and tandem ring opening/ring closing metathesis. In all cases the dendritic catalyst is highly active and the support of the dendrimer allows for recycling. Dendrimer **34** was employed in six sequential ring-closing reactions all with isolated yields of 87% or greater. The dendritic catalyst is separated from the reaction mixture via chromatography over silica gel. However, based on ^{1}H NMR spectroscopic analysis of the recovered dendrimer, there is a significant amount of Ru leaching. After the sixth cycle, only 41% of the original amount of Ru still remains bound to the dendrimer framework of **34**. While still very high, the observed yield decreased steadily in successive reactions. This leaching was suggested to be the result of backfolding of the arms of the dendrimer, limiting access of the styrenyl ether end group to the released Ru-carbene, preventing return. In the case of the more active metathesis catalyst in **35**, the amount

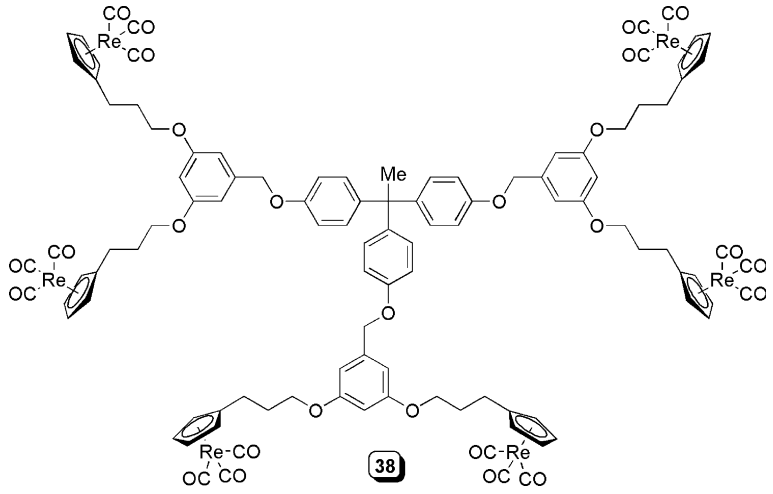

Fig. 16. Structure of Moss's Re containing dendrimer **38**.

of leaching is reduced but still, recovery of the monomeric Ru catalyst is more efficient.

Moss and coworkers [61] have recently reported the synthesis of a first generation organorhenium dendrimer **38** containing six $CpRe(CO)_3$ units in the periphery. Using methodology previously employed to assemble Fe and Ru dendrimers [5,6,20], the synthesis consists of the assembly of Fréchet-type wedges containing two rhenium centers and coupling them, through a benzylic bromide, to the 1,1,1-tris(4-hydroxyphenyl)ethane core. The structure of dendrimer **38** is shown in Fig. 16. The dendrimer was characterized by NMR spectroscopic studies and MALDI-TOF mass spectrometry. Attempts to oxidize the peripheral Re centers to catalytically active oxo-rhenium species were not successful.

Astruc and coworkers [62] have synthesized a dendrimer in which an arene RuCp* cationic functionality is incorporated. This work extends the large volume of complexes reported by Astruc in which a cationic arene FeCp moiety is used to activate the coordinated arene towards hexasubstitution [63]. This reaction was employed to generate star polymers and dendrimers incorporating a hexa-substituted benzene core. Indeed, the synthesis of the Ru containing compound **39** follows

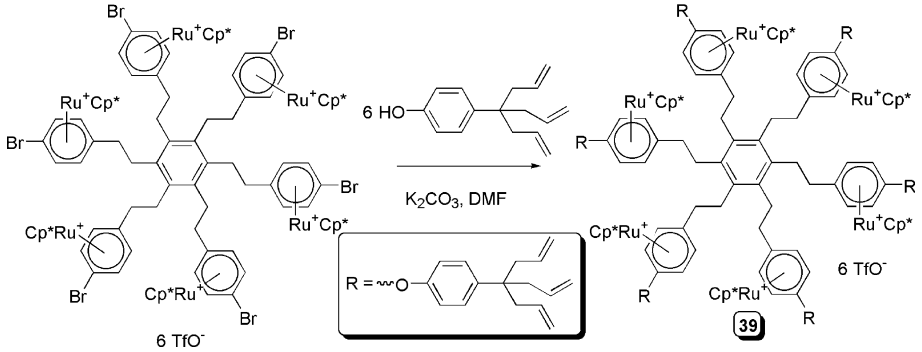

Scheme 11. Synthesis of Astruc's Ru arene dendrimer **39**.

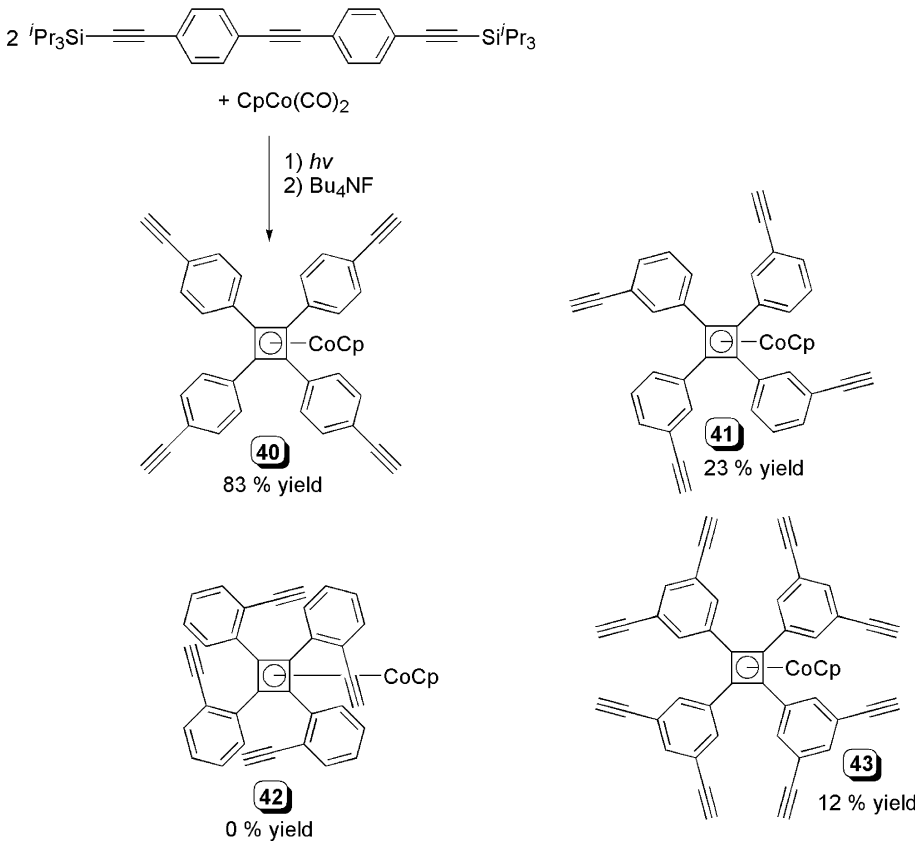

Scheme 12. Synthesis of Bunz's polyphenylacetylene cyclobutadienylcobaltocene compounds **40**–**43**.

similar reaction procedures. The incorporation of the cationic Ru fragment allows for selective activation of an aryl bromide towards nucleophilic substitution, a necessary step for dendrimer construction where the iron route failed. The final step of the synthesis of the dendrimer is shown in Scheme 11. The allyl functions in the dendrimer periphery may be employed for further reactivity for generation of extended structures.

3. Core functionalization of dendrimers with organometallic species

This type of dendrimer consists of an organometallic-based core with an organic-derived dendritic structure built up about the metal. In some senses, the dendrimer portion can be considered as an extremely large ligand to the metal center. However, the dendritic structure can provide additional features that other ligands cannot. Entrapment of an organometallic species at the core of a dendrimer can greatly influence the reactivity of the metal center by limiting interaction with the bulk solution and solutes and also limit or direct the access of substrates [10]. Also, the environment inside the dendrimer skeleton can be significantly different from the bulk solution, in polarity for example, and may alter reactivity of the organometallic.

Bunz and coworkers [64] have recently reported the synthesis of a number of polyphenylene dendrimers containing a cyclobutadienylCoCp functionality at the core. The necessary ethynyl phenyl starting materials were prepared using Pd-catalyzed Sonogashira type coupling

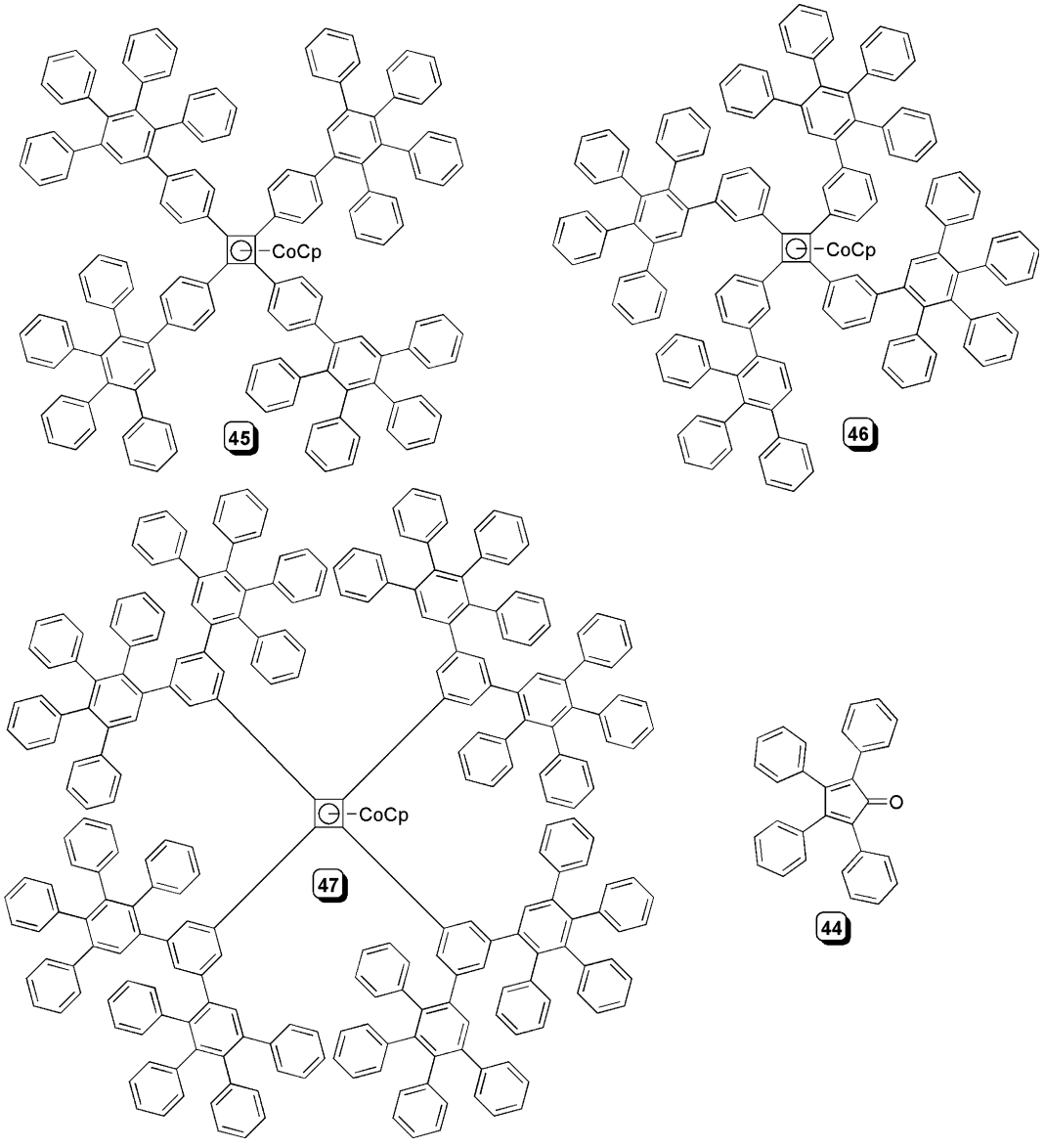

Fig. 17. Structure of Bunz's polyphenylene cyclobutadienylcobaltocene dendrimers **45**–**47**.

reactions in good yields. The Co-initiated [2 + 2] cycloaddition of the ethynyl units with $CpCo(CO)_2$ proceeded exclusively between the desired internal aryl alkynes. An example is given in Scheme 12. Steric protection of the terminal alkynes by the triisopropylsilyl groups inhibits reaction at these positions. However, the isolated yields of the cycloaddition reaction decreased with addition of steric bulk about the diarylalkyne, see Scheme 12. For example, shifting the position of the Si(*i*-Pr)$_3$-appended alkynyl moiety through *para*, *meta*, and *ortho* positions results in a decrease in yield of the cycloaddition reaction from 83%, 23% to 0% for dendrimers **40**, **41**, and **42**, respectively. The yields refer to the isolated product after removal of the Si(*i*-Pr)$_3$ protecting groups with Bu_4NF. The doubly substituted alkynylaryl **43** was obtained in 12% yield. To generate the dendritic structures, the deprotected terminal alkynes were reacted in a Diels–Alder cyclization with 2,3,4,5-tetraphenylcyclopentadienone **44** to generate dendrimers **45**–**47** shown in Fig. 17, following a procedure first exploited by Müllen and coworkers [65] for the synthesis of their polyphenylene dendrimers.

The dendrimers were characterized via ^1H and ^{13}C NMR spectroscopy, indicating complete formation of the desired structures; no terminal ≡C–H groups were detected. In the case of the largest species **47**, the room temperature ^1H NMR is broad and featureless, indicating restricted rotation of the sterically hindered aryl groups. Heating the NMR sample to 115 °C allows for free rotation and assignment of the spectra. Gel permeation chromatography (GPC) showed that the dendrimers were essentially monodisperse (M_w/M_n = 1.02–1.07), providing additional evidence for the lack of defects in the structures. There was, however, a significant difference in the retention time of the *meta* and *para* isomers in the GPC experiment, a somewhat unexpected result. Analysis of space-filling models shows that *para*-isomer **45** adopts a much more extended structure than the *meta* species **46**. This results in a much larger hydrodynamic volume for **45** and shorter retention time compared to **46**.

As the cyclobutadienylCpCo centers at the core of the dendrimers are electroactive, electrochemical experiments were performed to determine if the encapsulation of the metal center has an effect on its oxidation potential. For these systems, there were some small differences noted in that the larger dendrimers were slightly more difficult to oxidize. While this effect was quite small in solution (oxidation potentials were 0.80, 0.82 and 0.83 V for **45**, **46**, and **47**, respectively) they do suggest a small effect caused by the dendritic periphery and research is underway to construct thin films of these species to determine if the small effects observed can be amplified.

Kaifer and coworkers have installed a ferrocene in the core of branched amido dendrimers. The dendrimer structure is unsymmetrical in that only one side of the ferrocene is substituted, as shown in Fig. 18, and this has serious consequences on the electrochemical behaviour of the ferrocene unit. The zeroth, first, and second generation species of type **48** and **49** were constructed via a convergent approach by reaction of chlorocarbonylferrocene with the pre-formed macromolecular amine dendrons [66]. A single example of a symmetrical version **50** was also reported. The ester functions in the periphery of $\mathbf{G}_n\mathbf{48}$ were hydrolyzed to carboxylic acids to generated water-soluble dendrimers $\mathbf{G}_n\mathbf{49}$. All species were synthesized in good yield and thoroughly characterized via NMR, UV–Vis, and IR spectroscopy and MALDI-TOF mass spectrometry.

One of the well-known properties of ferrocenes is their ability to bind to the inside cavity of β-cyclodextrins (β-CD). These investigations were undertaken with these compounds but could only be performed on carboxylic acid-substituted dendrimers **49**, due to their solubility in water. The binding interaction was monitored by electrochemical means and clearly showed that the β-CD and the dendrimer bound ferrocene were forming inclusion complexes. There were, however, some differences when comparing the dendrimers of various generations. The accepted mechanism for electron transfer for ferrocene/β-CD complexes involves initial dissociation of the complex followed by the redox event. As such, the binding constants play an integral role in determining the voltametric response. As expected, the binding constants were found to rapidly decrease as the dendrimer generation increases. This result indicates that while the ferrocene is only singly substituted, the larger generation dendrimers have a significant impact on the steric environment about the electroactive center, which in turn blocks approach of the β-CD or significantly destabilizes the ferrocene/β-CD complex.

The ability to control the steric impact and orientation of the dendrimer with respect to the functionalities in the core is an important factor in potentially tuning the properties of the core group. In terms of electrochemical factors, the dendrimer can shield the ferrocene group and affect electron transfer process and therefore the orientation of the dendrimer with respect to the electrode surface can have important consequences. The Kaifer group has investigated the use of the carboxylic acid-adorned dendrimers $\mathbf{G}_n\mathbf{49}$ in this sense [67]. As the overall charge of the dendrimer can be completely controlled via alteration of pH, the orientation of the dendrimer towards an electrode surface may be influenced. At pH > 7, all the acid functions are fully ionized, imparting significant negative charge on the dendrimer. The aim of this study is to determine the influence of pH, and thus dendrimer charge, on the electrochemical parameters of the core-bound ferrocenes. Electrochemistry using gold beads as electrodes exhibited some changes of the $E_{1/2}$ values with various dendrimer generations

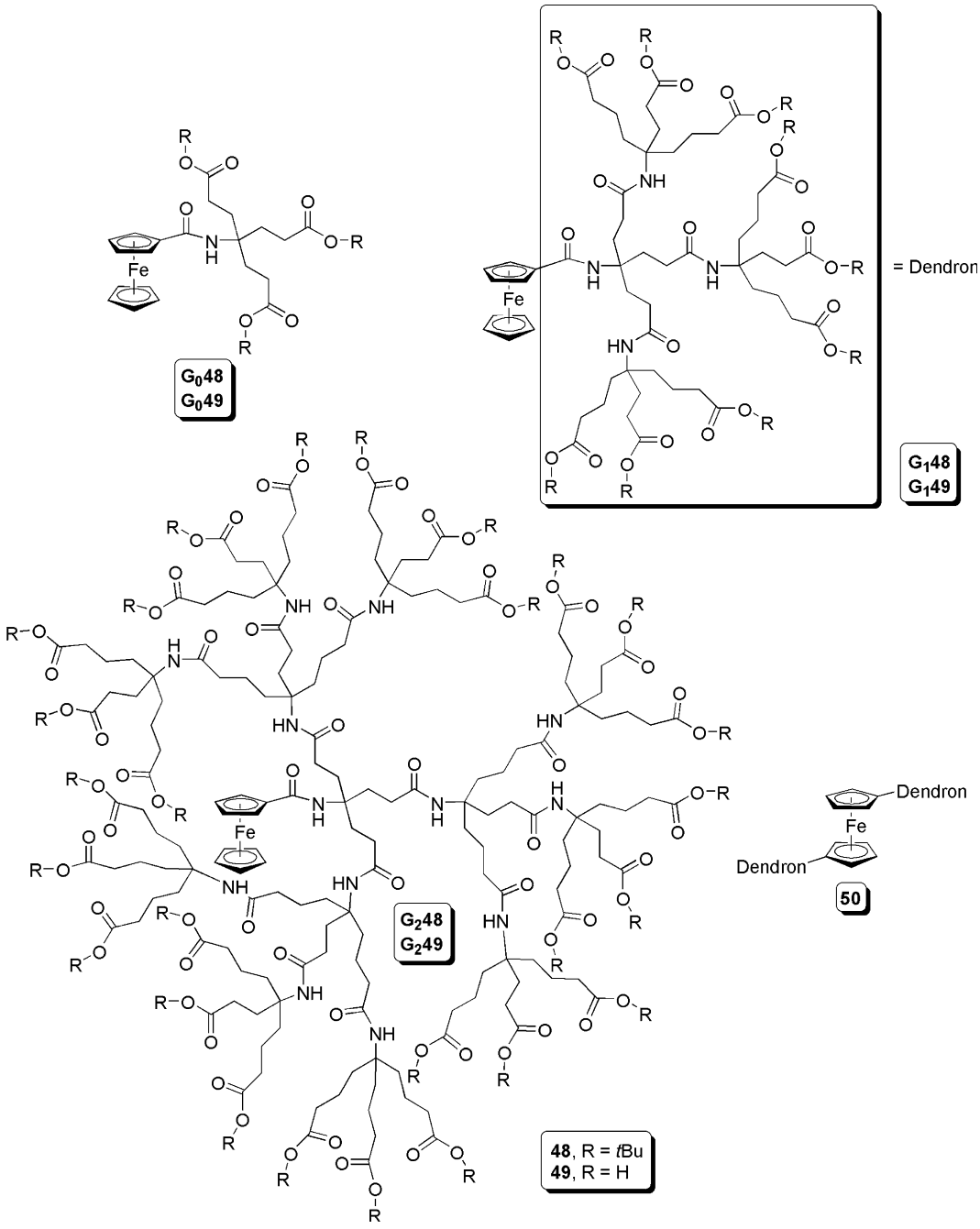

Fig. 18. Structure of Kaifer's off-center ferrocene dendrimers **48** and **49** and doubly substituted **50**.

(vide supra) but exhibited *no* pH dependence. To increase the overall charge of the electrode, gold nanoparticles covered with a thiolate monolayer incorporating cystamine residues were employed. The range of pH studied (3.0–7.4) ensures that the amino groups of the monolayer are positively charged during all experiments. Using the modified electrodes, a large dependence on the rate of electron transfer in the various generation dendrimers with pH was observed. While the zeroth generation dendrimer $\mathbf{G_0}\mathbf{49}$ exhibited very little change in the rate of electron transfer, the larger compounds showed much slower kinetics with increasing pH. Variations of three and four orders of magnitude in rate were apparent for $\mathbf{G_1}\mathbf{49}$ and $\mathbf{G_2}\mathbf{49}$, respectively. From this, it was postulated that at low pH, the uncharged dendrimer can freely rotate in solution and exhibit fast electron transfer behavior, as shown in Fig. 19. As the pH is increased, the developing charges in the dendrimer are electrostatically attracted to the modified electrode surface, restricting rotation and shielding the ferrocene from the electrode and impeding the electron transfer. While this behaviour is

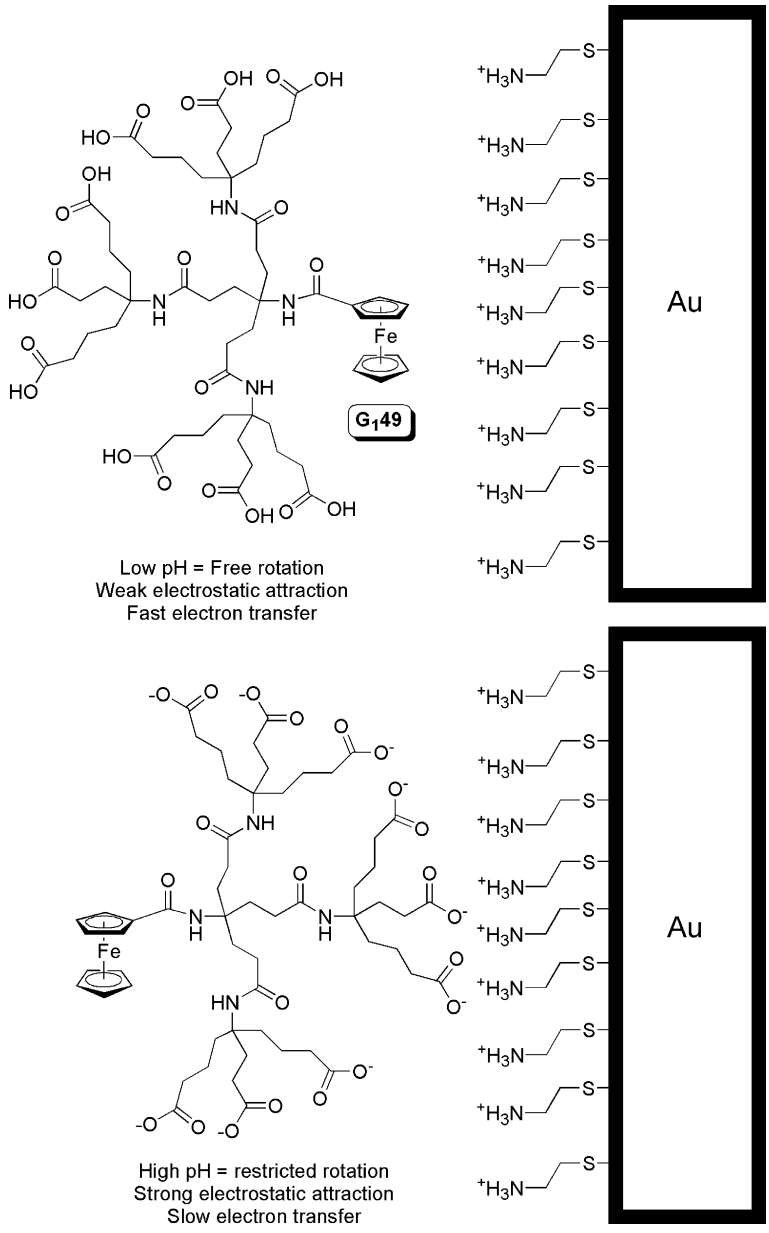

Fig. 19. Schematic representation of the interaction of Kaifer's off-center ferrocenyl dendrimer **$G_1$49** with a cystamine-treated Au electrode at low and high pH.

well known for biological redox active proteins, cytochrome *c* for example [68], this constitutes the first report of controlled orientational effects affecting electron transfer behavior in a completely synthetic system.

In additional work by Kaifer and coworkers [69], the electrochemical properties of the organic soluble dendrimers **G_n48** were investigated in CH_2Cl_2 solutions. It was observed that the $E_{1/2}$ values for the unsymmetric dendrimers become less positive, i.e., the oxidation of ferrocene to ferrocenium becomes more favoured, with increasing dendrimer generation. This result was notable as most of the systems reported to date show very small variations in the $E_{1/2}$ values. The main dendritic effect was the decrease of electrochemical reversibility due to slowing of the electron transfer rate. The $E_{1/2}$ values obtained were 0.63, 0.60 and 0.54 V (vs. Ag/AgCl) for **$G_0$48**, **$G_1$48** and **$G_2$48**, respectively. It was rationalized that inclusion within the dendrimer framework somehow stabilizes the positive charge of the oxidized ferrocenium species. This, however, does not hold for the symmetrical dendrimer **50** as the $E_{1/2}$ value *increases* to 0.73 V. While this was ascribed primarily to the effect of an additional electron withdrawing amido group, some other effects may also be in operation (vide infra). Also reported were *quantitative* values for the rate of

electron transfer (k^0), the first known rate values for electron transfer in a dendritic system. As expected, the smallest dendrimer **$G_0$48** exhibits the largest values for k^0 ($80 \pm 20 \times 10^3$ cm/s), indicating the fastest rate of electron transfer. Increasing generations significantly slowed the electron transfer process, $k^0 = 17 \pm 3$ and $9 \pm 2 \times 10^3$ cm/s for **$G_1$48** and **$G_2$48**, respectively, indicating that, even though the dendrimer is only attached to one side of the ferrocene, it can partially shield the core functionality. In the case of the symmetric system **50**, k^0 is approximately half the value for **$G_1$48**, again showing that the unsymmetrical dendrimer only partially protects the interior groups.

In terms of the effect of dendrimer generation and structure on the electrochemical behaviour of a core bound ferrocene, the group of Smith has studied the dendrimers of Kaifer as well as some structurally related systems to help elucidate the factors which cause the observed variations [70]. The main difference between the Smith dendrimers and those of Kaifer is the symmetric substitution about the ferrocene and the incorporation of an ether moiety in the branches. The dendrimers of Smith **G_n51**, depicted in Fig. 20, were also synthesized in a convergent fashion by the reaction of 1,1′-bis(chlorocarbonyl)ferrocene with the appropriate amino dendron using DMAP or NEt_3 as a base. The synthesis of larger systems via a convergent approach was impeded by the steric bulk of the dendrons; the second generation dendrimer **$G_2$51** could only be synthesized in relatively low yield (34%) and there were significant quantities of the mono-substituted product apparent by gel permeation chromatography. The products were analyzed by ^{1}H and ^{13}C NMR and IR spectroscopies as well as ESI-MS and CV experiments. For **$G_2$51**, preparative gel permeation chromatography was necessary to purify the disubstituted product from the mono.

Electrochemical investigations were performed in a range of different solvents and electrolyte concentrations. All three dendrimers studied show clearly reversible waves but, as with Kaifer, increasing dendrimer generation had a significant effect on the redox potential. In contrast to Kaifer, however, the oxidation potential, employing equivalent solvent and electrolyte, shifted to *more* positive values indicating a *destabilizing* dendritic effect for the ferrocenium cation. The minor differences in the composition of the dendrimer, incorporation of the ether linkages in the backbone for exam-

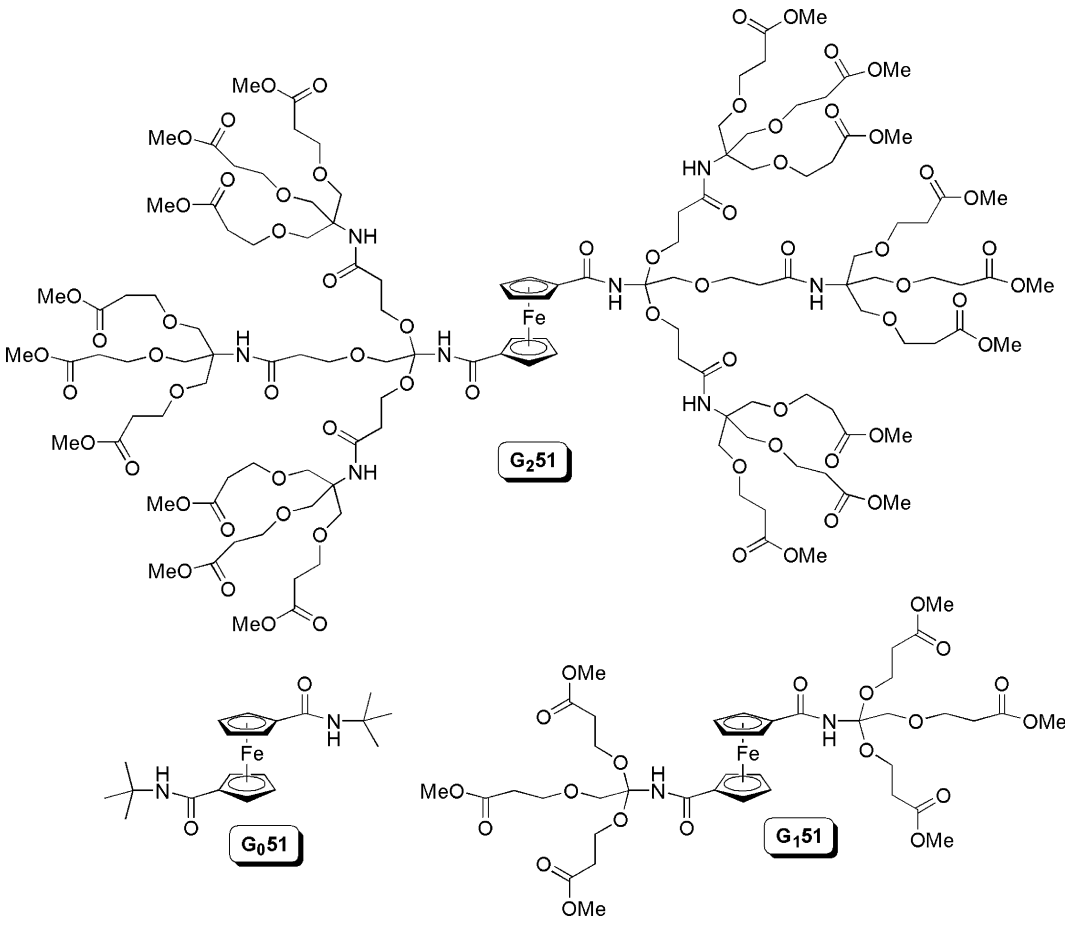

Fig. 20. Structure of Smith's polyamidoether ferrocenyl dendrimers **51**.

ple, should not account for such a dramatic reversal in trends and thus symmetrical or unsymmetrical substitution pattern about the ferrocene is the likely source of the observed effects. As illustrated by Kaifer, a symmetrical dendritic environment about the core results in more effective shielding of the core from external influences. This encapsulation results in the formation of a "micro environment" [10,71] about the core functionality that may be significantly different from the bulk solution.

The proposal put forward by Smith was that the dendritic microenvironment shields the core from stabilizing ion-ion interactions with the electrolyte. The effect of solvent polarity can also influence the redox potential. Experiments were performed to establish the polarity of the electrolyte/solvent combinations; a CH_2Cl_2 solution of 0.2 M $[Bu_4N][BF_4]$ has approximately the same polarity as butanenitrile. The effect of varying the concentration of electrolyte (0.125–1.0 M) clearly shows a large difference in redox potential for the zeroth generation dendrimer **$G_0$51**, with increasing electrolyte concentration stabilizing the oxidized species, with an $\Delta E_{1/2}$ of 0.60 V over the studied range. The effect of varying the electrolyte concentration is halved for **$G_1$51** ($\Delta E_{1/2}$ = 0.33 V). Encapsulation of the ferrocene is proposed to disfavour ion pairing of the ferrocenium cation with the electrolyte anions and thus increasing the redox potential.

However, the unsymmetrical dendrimers of Kaifer (**48** and **49**) exhibit a *stabilizing* influence for the oxidation of the core bound ferrocene. While it is obvious that the unsymmetric substitution does not shield the core as effectively as symmetric, the reasons for the stabilizing influence are somewhat unclear. Smith has proposed that H-bonding interactions may provide a stabilizing influence for the ferrocenium cation [70]. This interaction is not possible in the symmetrical systems due to the enormous steric size of the individual dendrons.

Raymo and coworkers [72] have encapsulated a ferrocene fragment within a carbohydrate dendrimer. This is expected to confer bio-stability and water solubility on the metallocene. The ferrocene moiety has a β-D-glucopyranosyl residue incorporated on one or both of the cyclopentadienyl rings. Both protected and deprotected carbohydrates have been synthesized. The dendrimer structures **52–59** are depicted in Fig. 21. All of the protected dendrimers (**52–55**) were synthesized via reaction of a pendent amine on the dendrons with a mono- or bis(chlorocarbonyl)ferrocene in the presence of Et_3N and isolated in good to excellent yields (54–92%). The deprotection reactions to generate the free carbohydrate dendrimers **56–59** were quantitative. The carbohydrate dendrimers were characterized via liquid secondary-ion mass spectrometry (LSI-MS) and multinuclear NMR spectroscopy; assignment of peaks was accomplished via two-dimensional NMR experiments. UV–Vis spectroscopy exhibited a low intensity absorption at λ_{max} = 440 nm, due to a d–d transition of the ferrocene fragment.

These dendrimers were also studied in the complexation of the cyclodextrin β-CD. In analogy to the results of Kaifer, the β-CD does complex with the mono-functionalized dendrimers, which was evident from NMR spectra, CV and circular dichroism experiments. As expected, increasing the dendrimer generation lowers the stability of the ferrocene β-CD complex. The doubly substituted species **57** and **59**, however, did not experience any complexation with β-CD as the substitution of both rings precludes formation of the inclusion complex.

The electrochemistry of the carbohydrate dendrimers corroborate the results found by Smith [70]. Increasing

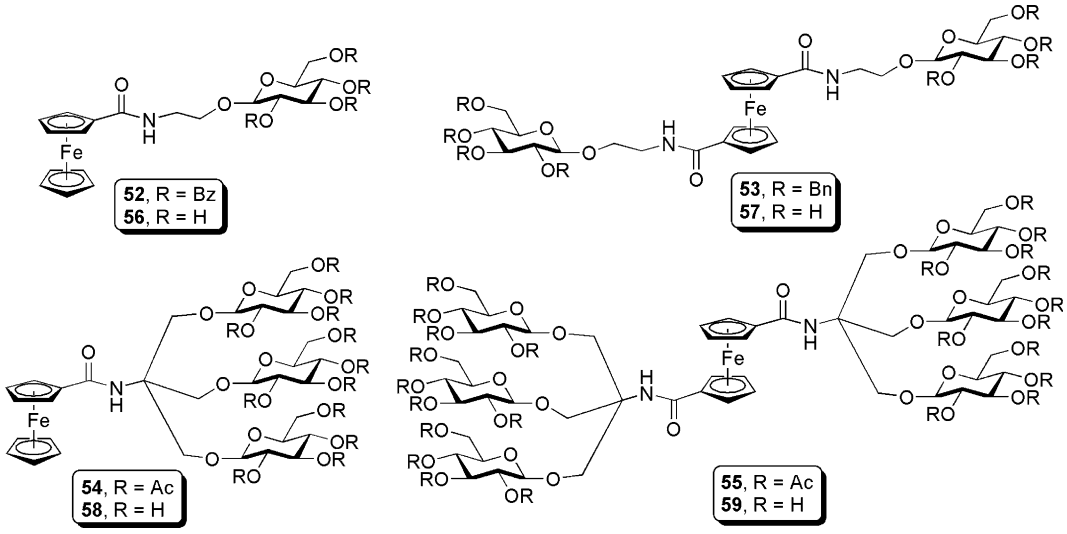

Fig. 21. Structures of Raymo and Credi's carbohydrate-substituted dendrimers **52–59**.

dendrimer generation destabilizes the ferrocenium cation and there is a larger difference between mono and di-substitution of the core. Di-substitution results in a more positive $E_{1/2}$ value due to introduction of an additional electron withdrawing amido group and to more effective isolation from solvent and electrolyte.

The unprotected derivative **59**, with a triply branched arm, exhibited a somewhat unusual differential pulse voltamogram. Two separate oxidation waves were observed at 0.54 and 0.64 V (vs. SCE) in water with a ratio of approximately 1:2, respectively. This was attributed to the presence of two distinct forms of the dendrimer in aqueous solution which impart different shielding character to the ferrocene core. The explanation for this is the presence of both *cisoid* and *transoid* configurational isomers in solution, shown in Fig. 22. The lower

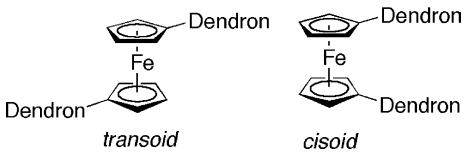

Fig. 22. *Cisoid* and *transoid* conformations in doubly substituted ferrocenyl dendrimers.

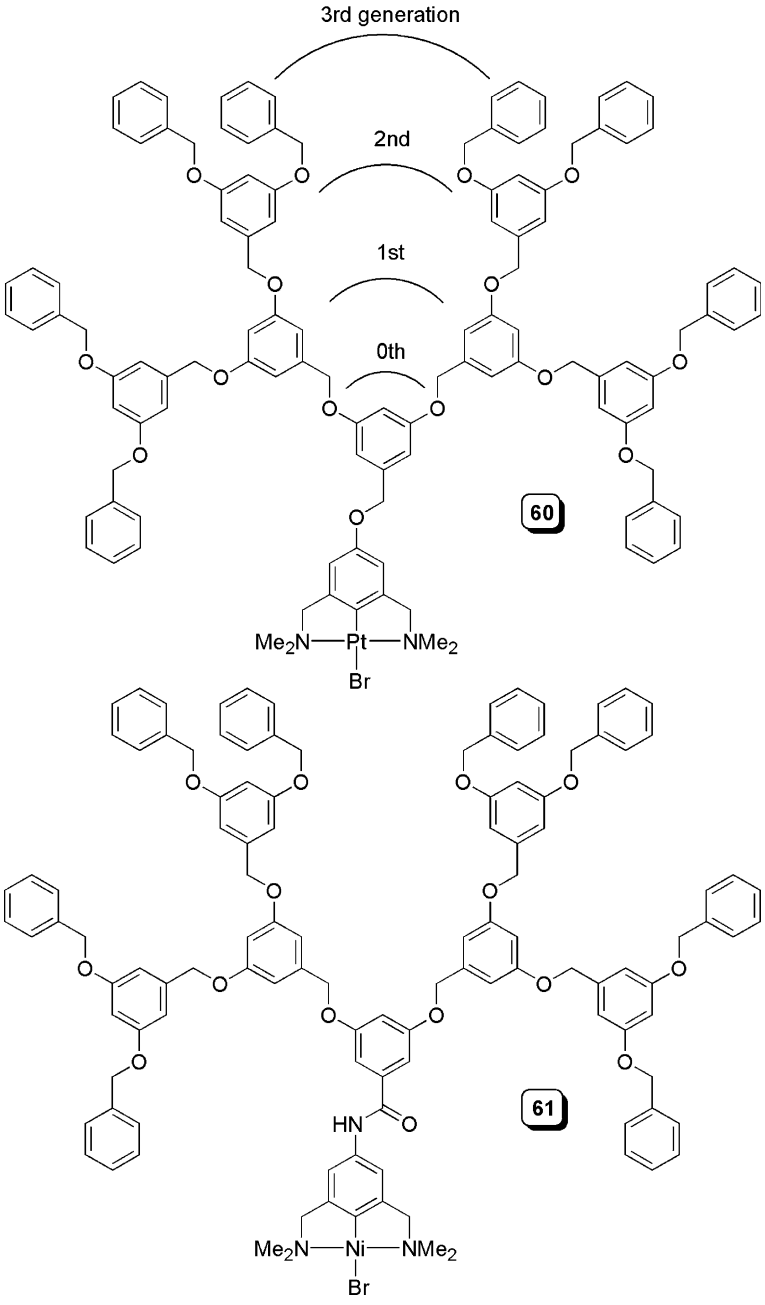

Fig. 23. Structures of van Koten's core-functionalized NCNPt (**60**) and NCNNi (**61**) pincer Fréchet-type dendrimers.

potential was attributed to the *cisoid* form, potentially stabilized via H-bonding interactions between the two dendrimer arms, as this will not as effectively shield the ferrocene from the bulk solution as the *transoid* species. The other species do not show this feature and a minimum steric size of the arms may be necessary for sufficient H-bonding interactions to stabilize the *cisoid* conformation.

The NCNPt function has also been incorporated into the core of a Fréchet-type dendritic wedge [73]. They were synthesized by reaction of 4-hydroxy-NCNPt with the appropriate benzylic bromide-substituted Fréchet-type dendritic wedges; yields were greater than 77% for dendrimers of type **60** to the third generation and the structures are shown in Fig. 23. The retention of the dendrimers in a nanofiltration experiment (membrane: SelRO-MPF-60) was monitored by colourimetric observation of the aforementioned SO_2 adducts of the NCNPt pincer functions in a CH_2Cl_2 solution saturated with SO_2. The degree of dendrimer leaching across the membrane barrier increased as a function of increasing dendrimer generation; $t_{1/2}$ values of 108 h, 300 h and >60 days for $\mathbf{G_1}\mathbf{60}$, $\mathbf{G_2}\mathbf{60}$, and $\mathbf{G_3}\mathbf{60}$, respectively, were established via UV–Vis spectroscopy of the SO_2 adducts. These findings underscore the fact that excessively large dendrimer generations need not be employed for successful membrane retention. Substitution of the NCNPt species with a related catalytically active NCNNi moiety in the third generation dendrimer **61** was employed to revisit the potential to separate products and the catalyst via nanofiltration in the Kharasch addition of CCl_4 to methyl methacrylate (see Section 2.2). As the active organometallic unit is ensconced in the core of the dendrimer, catalyst deactivation by the previously described radical coupling mechanism was not observed. Catalytic reactions using a membrane-capped vial were complete (>99% conversion) in 48 h; the somewhat longer reaction time compared to non-compartmentalized systems (4 h) was ascribed to restricted mass transfer. Catalyst removal was effected by removal of the vial from the reaction solution. This study showed that nanofiltration can be successfully employed with dendrimers-substituted NCN pincer systems and indicates that the use of vials loaded with different dendritic organometallic catalysts allows the execution of cascade-type synthesis in a single batch reactor.

4. Organometallic fragments in the dendrimer backbone

By far, this type of substitution, in which the organometallic species is incorporated within the dendrimer skeleton, is most rare. However, there are a multitude of dendrimers containing metal centers in every generation constructed by coordination chemistry. One of the best examples are dendrimers in which Ru(bipy) functions are present and act as antennae for the production of light harvesting dendrimers [74]. Also, one of the first reported dendrimers containing an organometallic functionality was of this type. Puddephatt and coworkers used successive oxidative addition/pyridine complexation to build up

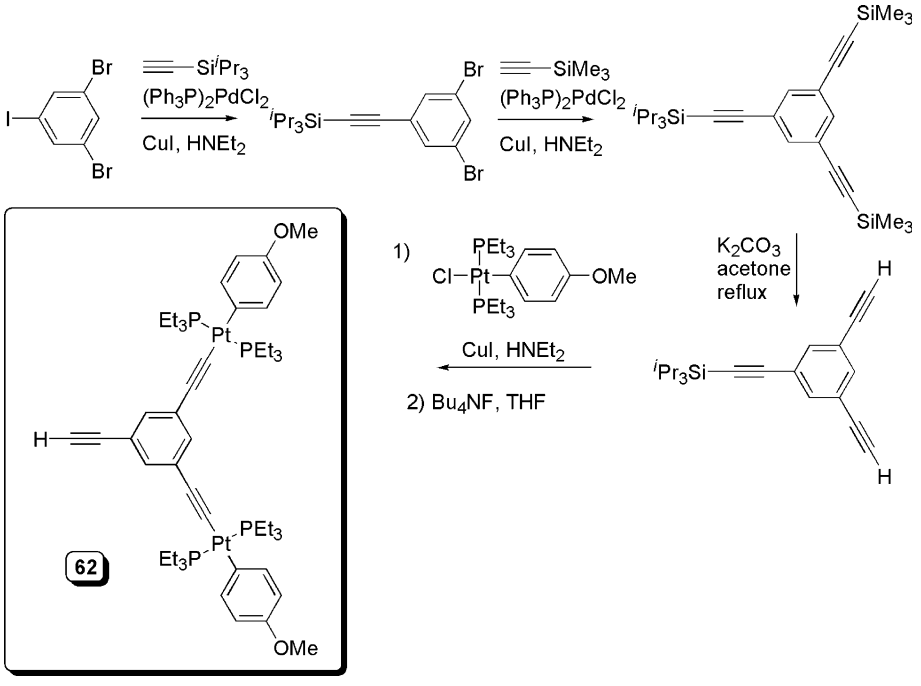

Scheme 13. Synthetic methodology of Takahashi for construction of Pt acetylide dendrimers.

a dendritic structure **1** (see Section 1). This "proof of principle" study, in which high yielding organometallic reactions were used to construct a dendritic structure, paved the way for the other successful investigations to come. The incorporation of organometallic species in each dendrimer generation may impart unique properties or reactivity on the novel species.

Takahashi has employed a platinum-acetylide functionality as the basis for the structure of numerous dendrimers [75,76]. Stang and coworkers concurrently reported the synthesis of essentially identical Pt acetylide dendrimers, employing a 1,3,5-substituted benzene core instead of mesityl [77]. These dendrimers were constructed up to the third generation. Recently, the Takahashi group has synthesized dendrons containing aryl-linked Pt-acetylide fragments throughout the structure and a pyridine functionality at the focal point of the wedge [78]. The general synthetic pathways and methodology for the Pt acetylide containing dendrons employs successive Cu(I)-catalyzed coupling reactions with PtCl groups and terminal acetylides. A typical synthesis of a first generation dendron **62** is shown in Scheme 13. Incorporation of a pyridine moiety, as in **63**, can be achieved by replacing the $Si(i\text{-}Pr)_3$ functionality in the scheme with a pyridine; the reaction methodology is tolerant of the pyridyl functionality. The isolated yield for the third generation pyridine containing dendron $\mathbf{G_3}$**63** was 44%. These wedges were subsequently attached to a tri-functional alkynyl metal core. Reaction of the core with 3 equivalents of the dendron and $NaB[m\text{-}C_6H_3(CF_3)_2]_4$ was investigated. Attempts to use Pt as the coordinating metal were unsuccessful; only partial ligand exchange was observed with the first generation dendron. Substitution to palladium allowed for rapid and quantitative synthesis of the first and second generation dendrimers. The first generation dendrimer $\mathbf{G_1}$**64** is shown in Scheme 14. However, no reaction was observed with the third generation dendron, presumably due to the steric size.

The most interesting feature of this class of dendrimers is that assembly of the dendrimer can be selectively switched on and off by the chemical conditions. This is the first reported example of reversible morphological control of the dendrimer structure by chemical stimuli. The Pd–pyridine interaction can be effectively disrupted by addition of excess Bu_4NCl, quantitatively re-generating the Pd–Cl core and three equivalents of the dendron **63**; this reaction sequence is depicted in Scheme 14. Re-complexation of the dendrimer is achieved via regeneration of the cationic Pd centers by $NaB[m\text{-}C_6H_3(CF_3)_2]_4$ in the presence of the dendrons. This cycle of dendrimer assembly/disassembly was repeated quantitatively three

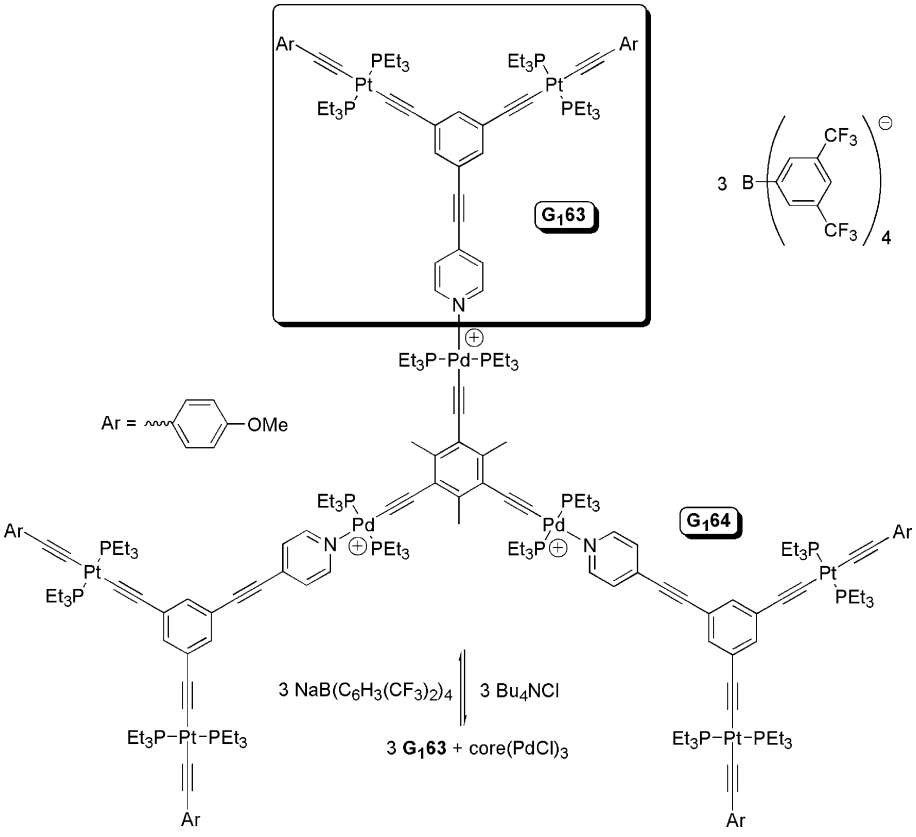

Scheme 14. Assembly/disassembly of Takahashi's pyridine-substituted Pt acetylide dendrimers **64**.

times with no degradation of the dendrimer or constituent components.

The Takahashi group has also, using similar synthetic methodology, coupled the Pt-acetylide dendrons to a Zn containing porphyrin [79]. While the synthetic yield of the peripherally Pt-decorated Zn porphyrin **65** is relatively low (29%), the coupling of the core with the various generation dendrons proceeds in quite good yields. For first, second and third generations of **66**, the yields of the completed dendrimers are 73%, 67% and 41%, respectively. A representative example of the porphyrin-centered Pt-acetylide dendrimer $\mathbf{G_1}\mathbf{66}$ is shown in Scheme 15.

Electronic absorption and fluorescence spectra were obtained for all the various generation dendrimers $\mathbf{G}_n\mathbf{66}$. Of particular note is the observation that there is energy transfer between the core porphyrin unit and the Pt-acetylides. Excitation of the MCLT band of the Pt-acetylide resulted in emission attributed to the porphyrin system. Also, excitation of the Soret band of the porphyrin leads to emission at wavelengths characteristic of the Pt-acetylide. While this effect was observed for all three generations of dendrimers, no effect was noted for a mixture of free dendron **62** and a porphyrin core **65**, strongly indicating that the charge transfer is intramolecular in nature.

In terms of construction of nanoscale materials, the Takahashi group has achieved the synthesis of very large dendritic structures based on the Pt-acetylide unit [80]. In contrast to the previous Pt-acetylide dendrimers, these species were generated using a divergent synthetic strategy; the synthesis of the zeroth and first generation dendrimers $\mathbf{G_0}\mathbf{68}$ and $\mathbf{G_1}\mathbf{68}$, respectively, are shown in Scheme 16. Simple deprotection of the Si(*i*-Pr)$_3$ group using Bu_4NF in THF to generate the terminal alkynes was followed by CuI-catalyzed coupling of the Pt–Cl containing dendron **67**. The inclusion of the three methyl groups in the core benzene was important for characterization of the dendrimers. They provided a convenient handle in the ^{1}H NMR spectrum in an area where no peaks due to other dendrimer fragments were present. Integration of these signals with respect to the other peaks gave evidence that the correct number of dendrons were successfully attached in each stage. Also, ^{1}H NMR spectroscopy was employed to monitor reactions via disappearance of the terminal acetylene CH signals.

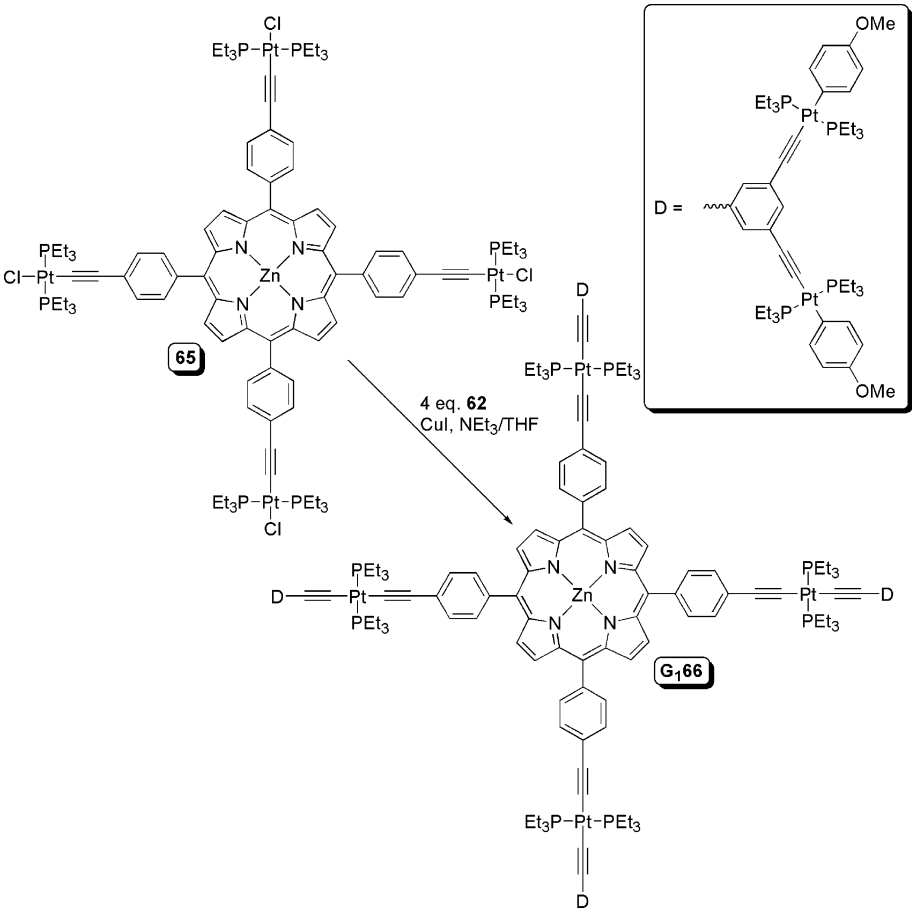

Scheme 15. Synthesis of Takahashi's Pt acetylide porphyrin dendrimers **66**.

Structures up to and including the sixth generation were reported; the largest dendrimer **$G_6$68** contains 189 Pt units per molecule and has a molecular weight of 139,750 g/mol. The nano-dimensional scale of **$G_6$68** was established via small angle neutron scattering experiments. Results indicate a molecular radius of 5.68 ± 0.02 nm, in good agreement with molecular modeling studies (diameter = 12 nm). The photophysical properties of these nanoscale molecules are currently under investigation.

Humphrey and coworkers [81,82] have reported the synthesis of a number of ruthenium-acetylide containing dendrimers. Essential to the construction of the dendrimers is the reaction of $Ru(dppe)_2Cl_2$ (dppe = 1,2-bis(diphenyl phosphino)ethane) with 1,3,5-tri(ethynyl)benzene. Even with excess Ru reagent, there is exclusive formation of the doubly Ru-substituted species **69**; it proved impossible to form the *tris* product under these conditions. This lack of reactivity of the third alkyne has been attributed to steric crowding and this

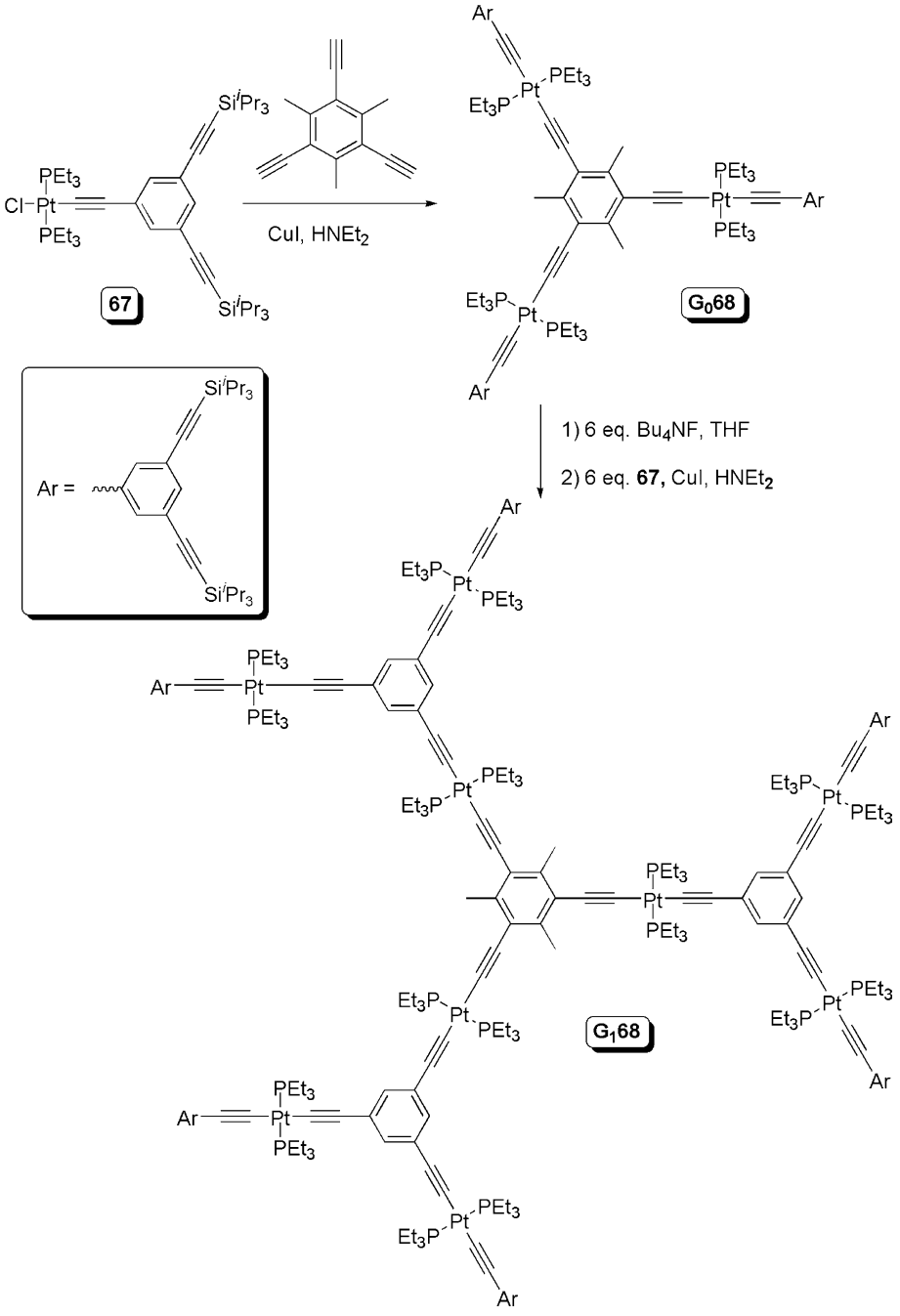

Scheme 16. Synthetic methodology of Takahashi for divergent construction of large Pt acetylide dendrimers **68**.

"steric control" has been effectively employed to generate a potential dendron. The synthesis of a dendrimer containing six ruthenium centers **70** is presented in Scheme 17.

To facilitate the incorporation of additional $Ru(dppe)_2$ fragments, a tri ruthenium core **71** was constructed by introduction of an arylethynyl spacer unit to overcome the steric crowding issues that limited the reaction described above [83]. This core was then successfully reacted with **69**, generating a new dendrimer **72**. The structures of the extended Ru acetylide dendrimers are shown in Fig. 24.

Some interesting non-linear optical (NLO) properties have been subsequently reported for these species. Increasing the size of the complexes does not affect optical transparency but the larger systems exhibit very high- and two-photon absorption cross-sections. These properties for complexes **70** and **72** are some of the largest reported to date.

The combination of these NLO properties and the demonstrated reversible electrochemical behavior of the Ru-acetylide functions [84] have also been investigated in terms of a possible reversible modulation of the optical properties of these species. The trimeric RuCl species undergoes reversible metal-centered redox processes ($Ru^{II/III}$) in solution. Upon oxidation, there appears an absorption band in the near IR region (893 nm). Also, oxidation has resulted in changes in the NLO properties as well.

Portnoy and coworkers [85] have reported the solid-phase synthesis of novel polythioether dendrimers that potentially form SCS type pincer coordination sites. First to fourth generation dendrimers were assembled via a three step iterative procedure to construct the individual dendritic shells, as shown in Scheme 18. The synthesis was performed using the Wang Bromo resin to initially attach the dendrimer to the resin via a thioether linkage by nucleophilic substitution. Reduction of the ester functions to alcohols, followed by chlorodehydroxylation complete the reaction sequence for a particular dendrimer generation. The synthesis of $\mathbf{G_4}$**73** was accomplished in 10 steps with an overall yield of 42% after detachment from the resin surface. The resin bound dendrimers were analyzed by gel-phase ^{13}C NMR spectroscopy in the bound state and by conventional solution phase multinuclear NMR spectroscopy and mass spectrometry after release from the resin surface. The detachment of the dendrimers

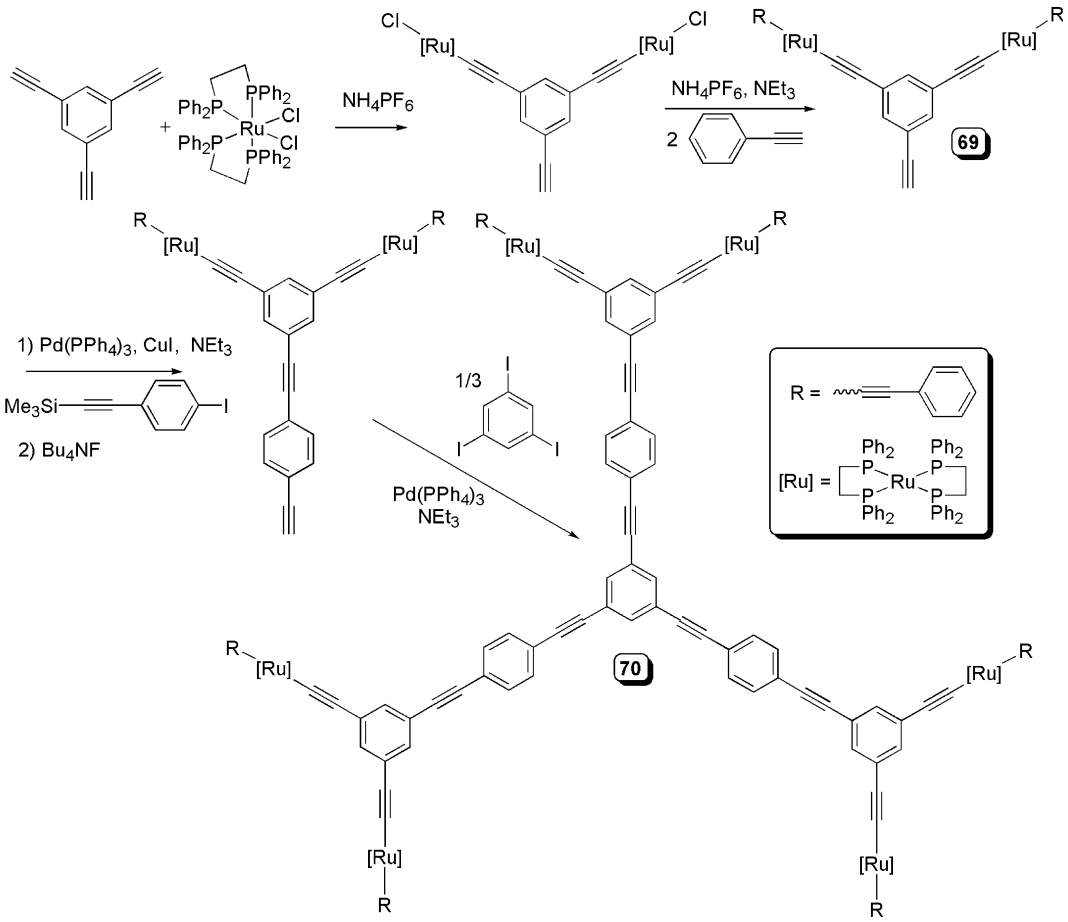

Scheme 17. Synthesis of Humphrey's Ru acetylide dendritic synthon **69** and dendrimer **70**.

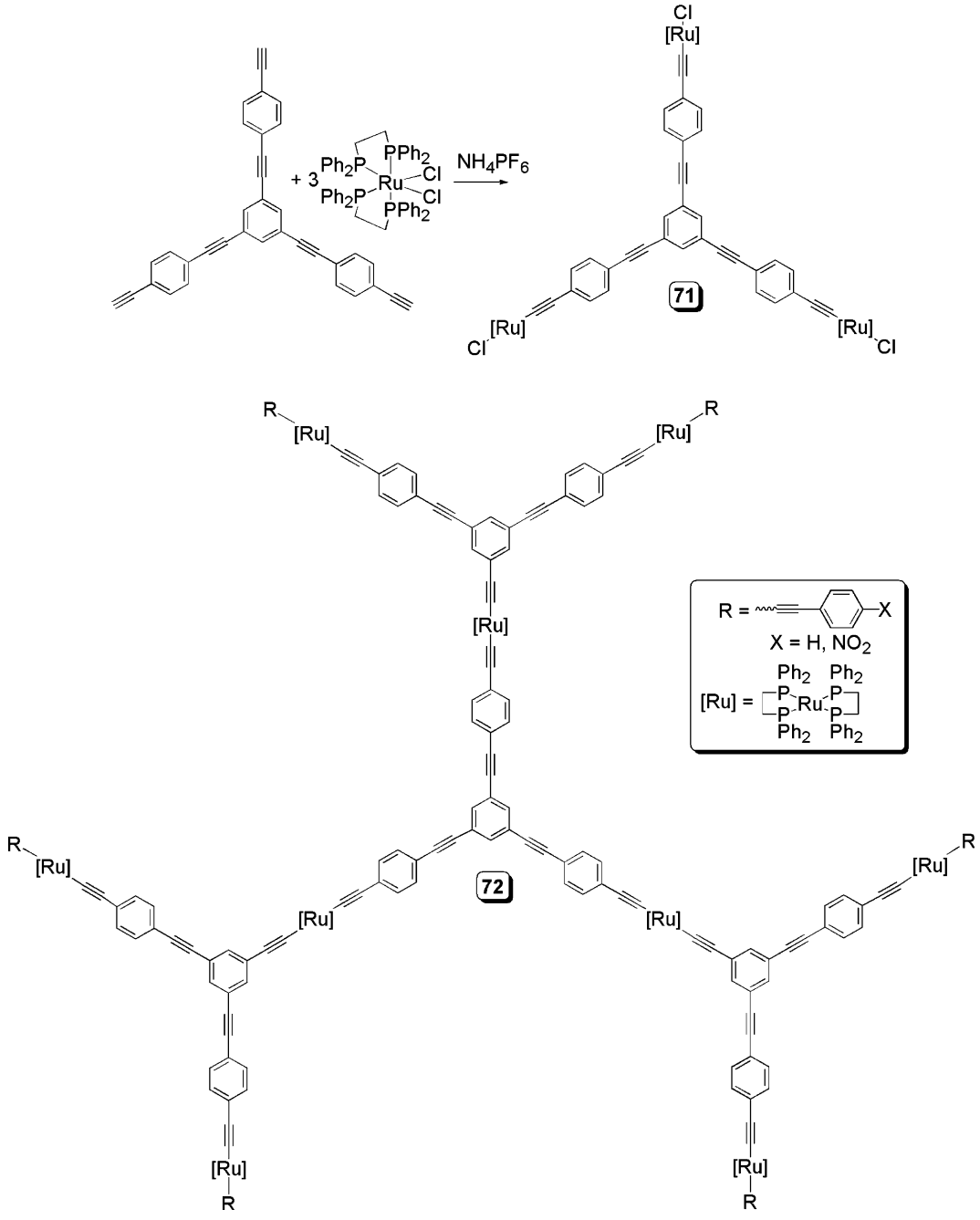

Fig. 24. Structure of Humphrey's extended Ru acetylide dendrimers **71** and **72**.

from the resin could be selectively achieved by acidolysis using trifluoroacetic acid. However, the cleavage reaction always occurred selectively within the resin framework and not between the linker and the dendron. This generates a 4-hydroxybenzyl-capped dendrimer core, as shown in Scheme 18.

Dendritic resins of $\mathbf{G_2}$**73** and $\mathbf{G_3}$**73** were tested for their ability to incorporate Pd centers and for their ability to perform as catalysts in the Heck reaction. Reaction of the dendrimer coated resins with $Pd(PhCN)_2Cl_2$ resulted in formation of deep red products, presumed to be of type **74**, see Fig. 25. The palladated dendrimers exhibited severely broadened NMR spectra for both resin bound and free dendrimers, which prevented full characterization. However, model SCSPd species **75,** shown in Fig. 25, were incorporated onto the Wang resin via an undecyl linker and these species were fully characterized in both the resin bound and detached forms. Both resin-attached species **74** and **75** were tested as recyclable catalyst in the Heck reaction of iodobenzene and methyl

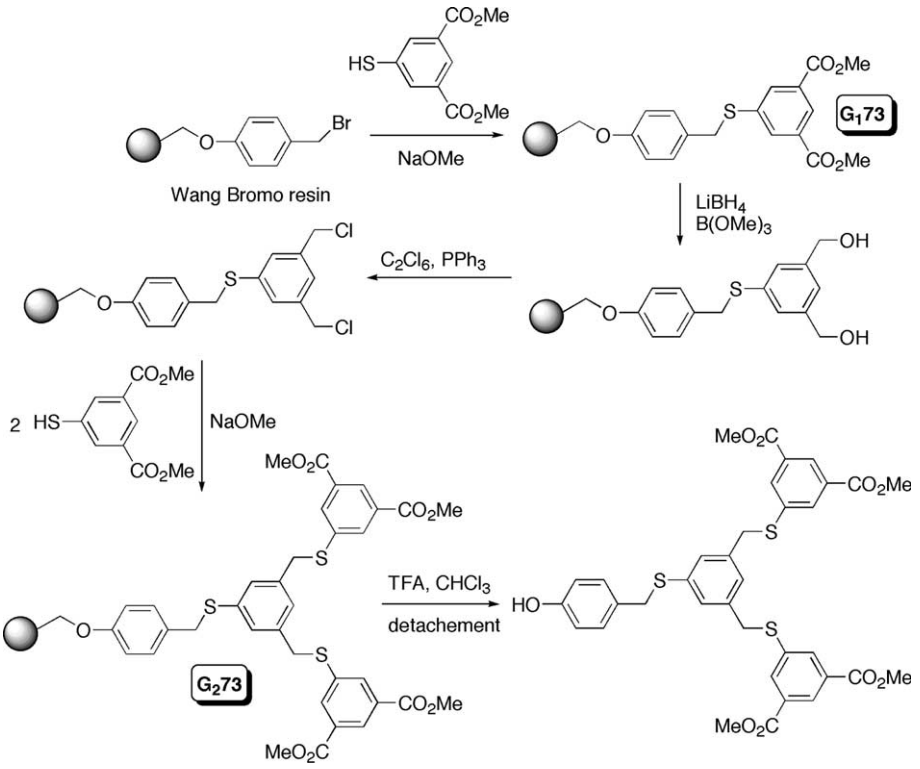

Scheme 18. Synthesis of Portnoy's resin bound SCS thioether dendrimers **73** and structure of resin-detached product.

acrylate. In preliminary catalytic testing with 2.5 mol% Pd loading in the reaction, dendrimer **$G_2$74** exhibited essentially quantitative conversion over two catalytic cycles.

5. Conclusions and future outlook

As shown through these selected examples, the field of dendrimer chemistry is still a rich and exciting area. The incorporation of organometallic fragments into dendrimer structures has permitted intimate probing of the properties and physical characteristics of the dendritic species. In particular, the introduction of stable, inert, but spectroscopically and chemically accessible ferrocene moieties have allowed for in-depth analysis of these systems which allows for development of a deeper understanding of the features needed to control dendrimer configuration and orientation, eminently important aspects for potential applications. The well-defined nature of dendrimers has also been exploited effectively to investigate the effect of site proximity on reactivity. Conversely, incorporation of organometallics within polymeric backbones can place the metal site in ill-defined environments and may not allow for precise structure/property relations to be developed [86] or may result in poor diffusion of substrates to the polymer bound active sites [87]. Also, dendrimers incorporating organometallic species in each generation have shown interesting physical and spectroscopic properties distinct from monomeric species. Finally, the robustness of the metal carbon bond within the organometallic fragments prevents leaching of the metal from the metallo-dendritic system.

There are some common trends that can be formulated from analysis of the properties of the various types of dendrimers. For peripherially substituted dendrimers, the high concentration of metal centers may or may not lead to distinct reactivity differences from monomeric counterparts. In the case of ferrocenes substituted dendrimers, there is often assumed to be no interaction of the electroactive centers as only one redox potential is generally observed, except in specially designed cases such as **14**. However, these effects can exhibit cooperative properties with the adjacent metal centers acting to amplify reactivity, as in $CpWCO_2Me$ functionalized dendrimers **32** for DNA scission experiments. Destructive interactions, such as deactivation of catalysts by formation of metal–metal bonds in NCNNi dendrimers **24**–**26**, can also be enhanced. In contrast, encapsulation of organometallic fragments within dendrimer cores isolates the metal center from association with other metal centers or with solvents. For example, rates of electron transfer for ferrocenes dendrimers **48** and **50** were found to precipitously decrease with increasing dendrimer generation. These isolation effects can also lead to advantageous reactivity or increased stability of the metal centers. This increased stability allowed for the isolation and reuse of dendritic catalysts **61** in the Kharasch addition.

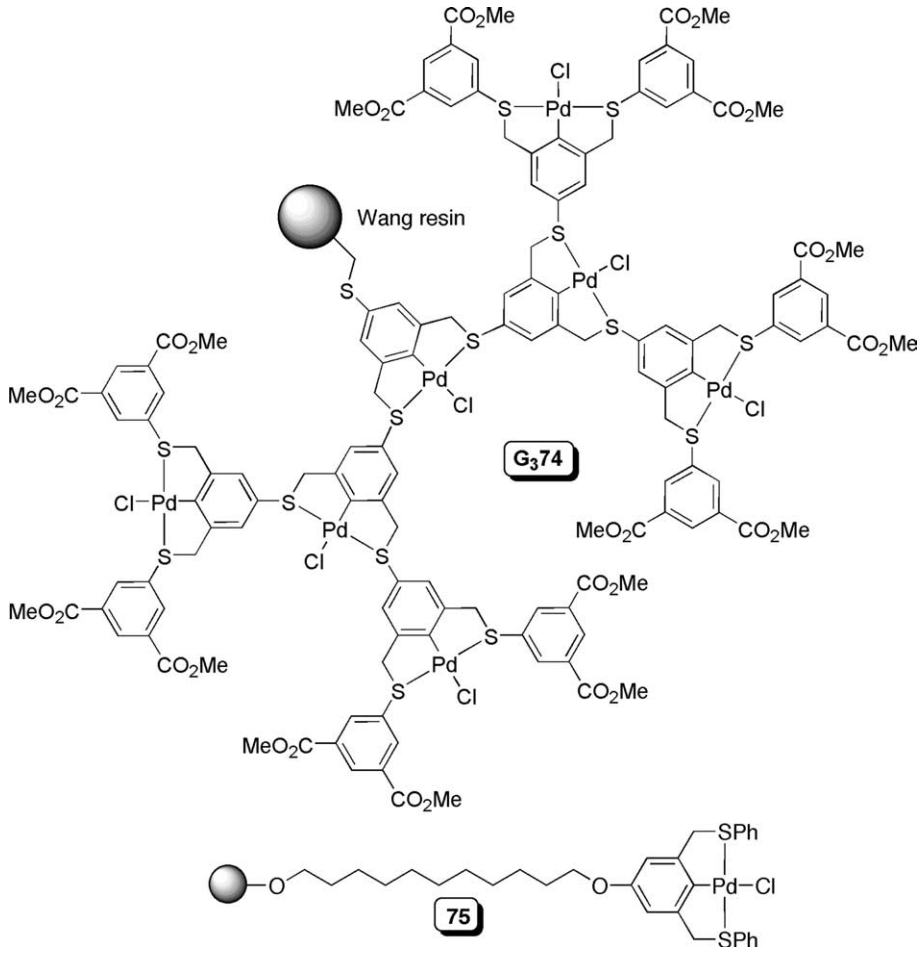

Fig. 25. Structure of Portnoy's third generation resin bound dendritic SCSPd catalyst $\mathbf{G_3 74}$ and model species **75**.

So where do we go from here? Dendrimers have assuredly progressed from esthetically pleasing, synthetic curiosities to a powerful tool in the chemist's repertoire. The synthetic strategies for incorporation of organometallic species into the core or periphery of dendrimers are now well established. Commercially available dendritic skeletons [88] or rapid, well-developed synthetic routes to dendrimers or potential dendrons are readily available. The main challenge now is the application of these species in the development of practical uses that will impact the chemical community or general population at large. In our view, dendrimers can act as the proving ground for new types of immobilized species. For example, fundamental research on the properties and characteristics and the fine-tuning of a catalyst or sensor can be performed using dendrimers as their highly symmetrical structures allow for common characterization techniques, such as NMR spectroscopy, to be employed. The lessons learned from the dendritic experiments can then be applied to the generation of economically or commercially more viable hyper-branched polymer or traditional polymer (polystyrene for example) systems. If differing reaction modalities are observed between the dendrimer and polymer, then the uniformity of sites imparted by the dendritic structure is necessary for a particular application. However, the dendrimer system retains some of the favourable characteristics of the polymer, such as recyclibility.

One of the main thrusts of modern chemistry is to limit the environmental impact of research and industry. Dendrimers can be separated by nanofiltration techniques and thus recycled or reused, an obvious benefit towards the development of "green" chemical processes. Catalyst compartmentalization and immobilization is also an important area as this allows for the development of continuous flow cascade reactions or formulation of "lab on a chip" devices. Also, dendrimer-functionalized electrodes or surfaces have seen some potential uses as selective sensors. For dendrimers containing organometallic species in each generation, new synthetic methodologies and selective high yielding reactions are needed to expand this field. As shown, these highly metallated compounds can have interesting properties, but research in this area is not as developed as others. One practical consequence of incorporation of a high degree of metallated

species throughout the dendrimer structure is that microscopic techniques, such as TEM, no longer require the addition of a staining agent. Further development of these and other fields will continue to push the utility and applicability of dendrimers and organometallic dendrimer species.

Acknowledgement

The Natural Sciences and Engineering Research Council of Canada (NSERC, post-doctoral fellowship, P.A.C.) and the National Research School Combination Catalysis (NRSC-C, R.J.M.K.G.) are gratefully thanked for financial support.

References

[1] G.R. Newkome, C.N. Moorefield, F. Vögtle, Dendritic Molecules. Concepts, Synthesis, Perspectives, Wiley-VCH, Cambridge, 1996.
[2] G.R. Newkome, C.N. Moorefield, F. Vögtle, Dendrimer and Dendrons. Concept, Synthesis and Application, Wiley-VCH, Weinheim, 2001.
[3] A.W. Bosman, E.W. Jansen, E.W. Meijer, Chem. Rev. 99 (1999) 1665.
[4] J.-P. Majoral, A.-M. Caminade, Chem. Rev. 99 (1999) 845.
[5] M.A. Hearshaw, J.R. Moss, Chem. Commun. (1999) 1.
[6] I. Cuadrado, M. Morán, C.M. Casado, B. Alonzo, J. Losada, Coord. Chem. Rev. (1999) 395.
[7] D. Astruc, F. Chardac, Chem. Rev. 101 (2001) 2991.
[8] G.E. Oosterom, J.N.H. Reek, P.C.J. Kamer, P.W.N.M. van Leeuwen, Angew. Chem. Int. Ed. 40 (2001) 1828.
[9] R. Kreiter, A.W. Kleij, R.J.M. Klein Gebbink, G. van Koten, Top. Curr. Chem. 217 (2001) 593.
[10] S. Hecht, J.M.J. Fréchet, Angew. Chem. Int. Ed. 40 (2001) 74.
[11] L.J. Twyman, A.S.H. King, I.K. Martin, Chem. Soc. Rev. 31 (2002) 69.
[12] R. van Heerbeek, P.C.J. Kamer, P.W.N.M. van Leeuwen, J.N.H. Reek, Chem. Rev. 102 (2002) 3717.
[13] S. Achar, R.J. Puddephatt, Angew. Chem. Int. Ed. Engl. 33 (1994) 847.
[14] S. Achar, R.J. Puddephatt, J. Chem. Soc., Chem. Commun. (1994) 1895.
[15] S. Achar, J.J. Vittal, R.J. Puddephatt, Organometallics 15 (1996) 43.
[16] J.W.J. Knapen, A.W. van der Made, J.C. De Wilde, P.W.N.M. van Leeuwen, P. Wijkens, D.M. Grove, G. van Koten, Nature 372 (1994) 659.
[17] For some examples see: M. Dasgupta, M.B. Peori, A.K. Kakkar, Coord. Chem. Rev. 233–234 (2002) 223.
[18] R.M. Crooks, M.Q. Zhao, L. Sun, V. Chechik, L.K. Yeung, Acc. Chem. Res. 34 (2001) 181.
[19] Y. Niu, R.M. Crooks, C. R. Chem. 6 (2003) 1049.
[20] S. Serroni, S. Campagna, F. Puntoriero, C. Di Pietro, N.D. McClenaghan, F. Louseau, Chem. Soc. Rev. 30 (2001) 367.
[21] E. Kim, K. Kim, H. Yang, Y.T. Kim, J. Kwak, Anal. Chem. 75 (2003) 5665.
[22] W. Fan, J. Li, J. Han, US Patent Appl. 114776 (2002).
[23] M.-C. Daniel, J. Ruiz, D. Astruc, J. Am. Chem. Soc. 125 (2003) 1150.
[24] (a) J.F.G.A. Jansen, E.M.M. de Brabander-van den Berg, E.W. Meijer, Science 265 (1994) 1226;
(b) J.F.G.A. Jansen, E.W. Meijer, J. Am. Chem. Soc. 117 (1995) 4417.
[25] S.C. Zimmerman, F. Zeng, D.E.C. Reichert, S.V. Kolotuchin, Science 271 (1996) 1095.
[26] C. Valério, J.-L. Fillaut, J. Ruiz, J. Guittard, J.-C. Blais, D. Astruc, J. Am. Chem. Soc. 119 (1997) 2588.
[27] A.-M. Caminade, V. Maraval, R. Laurent, C.-O. Turrin, P. Sutra, J. Leclaire, L. Griffe, P. Marchand, C. Baudoin-Dehoux, C. Rebout, J.-P. Majoral, C. R. Chim. 6 (2003) 791.
[28] C.-O. Turrin, J. Chiffre, D. de Montauzon, G. Balavoine, E. Manoury, A.-M. Caminade, J.-P. Majoral, Organometallics 21 (2002) 1891.
[29] C.-O. Turrin, J. Chiffre, J.C. Daran, D. de Montauzon, A.-M. Caminade, E. Manoury, G. Balavoine, J.-P. Majoral, Tetrahedron 57 (2001) 2521.
[30] A. Togni, C. Breutel, A. Schnyder, F. Spindler, H. Landert, A. Tijani, J. Am. Chem. Soc. 116 (1994) 4062.
[31] C. Köllner, B. Pugin, A. Togni, J. Am. Chem. Soc. 120 (1998) 10274.
[32] R. Schneider, C. Köllner, I. Weber, A. Togni, Chem. Commun. (1999) 2415.
[33] A. Togni, N. Bieler, U. Burckhardt, C. Köllner, G. Pioda, R. Schneider, A. Schyder, Pure Appl. Chem. 71 (1999) 1531.
[34] I. Cuadrado, C.M. Casado, B. Alonso, M. Morán, J. Losada, V. Belsky, J. Am. Chem. Soc. 119 (1997) 7613.
[35] J. Alvarez, T. Ren, A.E. Kaifer, Organometallics 20 (2001) 3543.
[36] A. Salmon, P. Jutzi, J. Organomet. Chem. 637–639 (2001) 595.
[37] T. Chuard, M.-T. Béguin, R. Deschenaux, C. R. Chim. 6 (2003) 959.
[38] C.M. Casado, B. González, I. Cuadrado, B. Alonso, M. Morán, J. Losada, Angew. Chem. Int. Ed. 39 (2000) 2135.
[39] S. Sengupta, Tetrahedron Lett. 44 (2003) 7281.
[40] (a) C. Galliot, D. Prévoté, A.-M. Caminade, J.-P. Majoral, J. Am. Chem. Soc. 117 (1995) 5470;
(b) M. Slany, M. Bardají, M.-J. Casnove, A.-M. Caminade, J.-P. Majoral, J. Am. Chem. Soc. 117 (1995) 9764.
[41] V. Chandrasekhar, G.T.S. Andavan, S. Nagendran, V. Krishnan, R. Azhakar, R.J. Butcher, Organometallics 22 (2003) 976.
[42] A.W. Kleij, R.A. Gossage, J.T.B.H. Jastrzebski, J. Boersma, G. van Koten, Angew. Chem. Int. Ed. 39 (2000) 176.
[43] A.W. Kleij, R.A. Gossage, R.J.M. Klein Gebbink, N. Brinkmann, E.J. Reijerse, U. Kragl, M. Lutz, A.L. Spek, G. van Koten, J. Am. Chem. Soc. 122 (2000) 12112.
[44] A.W. Kleij, H. Kleijn, J.T.B.H. Jastrzebski, W.J.J. Smeets, A.L. Spek, G. van Koten, Organometallics 18 (1999) 268.
[45] A.W. Kleij, H. Kleijn, J.T.B.H. Jastrzebski, A.L. Spek, G. van Koten, Organometallics 18 (1999) 277.
[46] M. Albrecht, R.A. Gossage, M. Lutz, A.L. Spek, G. van Koten, Chem. Eur. J. 6 (2000) 1431.
[47] M. Albrecht, G. van Koten, Angew. Chem. Int. Ed. 40 (2001) 3750.
[48] M. Albrecht, M. Lutz, A.L. Spek, G. van Koten, Nature 406 (2000) 970.
[49] M. Albrecht, M. Schlupp, J. Bargon, G. van Koten, Chem. Commun. (2001) 1874.
[50] (a) W.T.S. Huck, F.C.J.M. van Veggel, D.N. Reinhoudt, Angew. Chem. Int. Ed. Engl. 35 (1996) 1213;
(b) W.T.S. Huck, R. Hulst, P. Timmerman, F.C.J.M. van Veggel, D.N. Reinhoudt, Angew. Int. Ed. Engl. 36 (1997) 1006;
(c) W.T.S. Huck, F.C.J.M. van Veggel, D.N. Reinhoudt, New J. Chem. 22 (1998) 165;
(d) H.-J. van Manen, R.H. Fokkens, F.C.J.M. van Veggel, D.N. Reinhoudt, Eur. J. Org. Chem. 18 (2002) 3189;
(e) For a current review see: H.-J. van Manen, F.C.J.M. van Veggel, D.N. Reinhoudt, Top. Curr. Chem. 217 (2001) 121.
[51] W.T.S. Huck, B. Snellink-Ruël, F.C.J.M. van Veggel, D.N. Reinhoudt, Organometallics 16 (1997) 4287.

[52] R. van de Coevering, M. Kuil, R.J.M. Klein Gebbink, G. van Koten, Chem. Commun. (2002) 1636.
[53] R. van de Coevering, A.P. Alfers, E. Martinez Viviente, P.S. Pregosin, R.J.M. Klein Gebbink, G. van Koten, in preparation.
[54] A.L. Hurley, D.L. Mohler, Org. Lett. 2 (2000) 2745.
[55] S.B. Garber, J.S. Kingsbury, B.L. Gray, A.H. Hoveyda, J. Am. Chem. Soc. 122 (2000) 8168.
[56] R.H. Grubbs (Ed.), Handbook of Metathesis, Wiley-VCH, Weinheim, 2003.
[57] T.M. Trinka, R.H. Grubbs, Acc. Chem. Res. 34 (2001) 18.
[58] R.R. Schrock, A.H. Hoveyda, Angew. Chem. Int. Ed. 42 (2003) 4592.
[59] S.J. Connon, S. Blechert, Angew. Chem. Int. Ed. 42 (2003) 1900.
[60] M. Ahmed, A.G.M. Barrett, D.C. Bradstock, S.M. Cramp, P.A. Procopiou, Tetrahedron Lett. 40 (1999) 8657.
[61] I.J. Mavunkal, J.R. Moss, J. Basca, J. Organomet. Chem. 593–594 (2000) 361.
[62] B. Alonso, J.-C. Blais, D. Astruc, Organometallics 21 (2002) 1001.
[63] For a recent overview of this work see: D. Astruc, Pure Appl. Chem. 75 (2003) 461, and references cited therein.
[64] S.M. Waybright, K. McAlpine, M. Laskoski, M.D. Smith, U.H.F. Bunz, J. Am. Chem. Soc. 124 (2002) 8661.
[65] M.D. Watson, A. Fechtenkötter, K. Müllen, Chem. Rev. 101 (2001) 1267.
[66] C.M. Cardona, T.D. McCarley, A.E. Kaifer, J. Org. Chem. 65 (2000) 1857.
[67] Y. Wang, C.M. Cardona, A.E. Kaifer, J. Am. Chem. Soc. 121 (1999) 9756.
[68] For an example of this phenomena see: A.E. Kamsi, J.M. Wallace, E.F. Bowden, S.M. Binet, R.J. Linderman, J. Am. Chem. Soc. 120 (1998) 225.
[69] C.M. Cardona, A.E. Kaifer, J. Am. Chem. Soc. 120 (1998) 4023.
[70] D.L. Stone, D.K. Smith, P.T. McGrail, J. Am. Chem. Soc. 124 (2002) 856.
[71] The initial concept of dendritic "micro environments" were presented in: C.J. Hawker, K.L. Wooley, J.M.J. Fréchet, J. Am. Chem. Soc. 115 (1993) 4375.
[72] P.R. Ashton, V. Balzani, M. Clemente-León, B. Colonna, A. Credi, N. Jayaraman, F.M. Raymo, J.F. Stoddart, M. Venturi, Chem. Eur. J. 8 (2002) 673.
[73] M. Albrecht, N.J. Hovestad, J. Boersma, G. van Koten, Chem. Eur. J. 7 (2001) 1289.
[74] (a) J. Issberner, F. Vogtle, L. deCola, V. Balzani, Chem. Eur. J. 3 (1997) 706;
(b) For recent developments in the field see:V. Balzani, P. Ceroni, A. Juris, M. Venturi, S. Campagna, F. Puntoriero, S. Serroni, Coord. Chem. Rev. 219 (2001) 545;
(c) V. Balzani, P. Ceroni, M. Maestri, C. Saudan, V. Vicinelli, Top. Curr. Chem. 228 (2003) 159;
(d) V. Balzani, F. Vogtle, C. R. Chim. 6 (2003) 867.
[75] K. Onitsuka, M. Fugimoto, N. Ohshiro, S. Takahashi, Angew. Chem. Int. Ed. 38 (1999) 689.
[76] K. Onitsuka, S. Takahashi, Top. Curr. Chem. 228 (2003) 39.
[77] S. Leininger, P.J. Stang, S. Huang, Organometallics 17 (1998) 3981.
[78] K. Onitsuka, A. Iuchi, M. Fugimoto, S. Takahashi, Chem. Commun. (2001) 741.
[79] K. Onitsuka, H. Kitajima, M. Fugimoto, A. Iuschi, F. Takei, S. Takahashi, Chem. Commun. (2002) 2576.
[80] K. Onitsuka, A. Shimizu, S. Takahashi, Chem. Commun. (2003) 280.
[81] S.K. Hurst, M.P. Cifuentes, M.G. Humphrey, Organometallics 21 (2002) 2353.
[82] A.M. McDonagh, C.E. Powell, J.P. Morrall, M.P. Cifuentes, M.G. Humphrey, Organometallics 22 (2003) 1402.
[83] M.G. Humphrey, C.E. Powell, M.P. Cifuentes, J.P. Morrall, M. Samoc, Polymer Preprints 45 (2004) 367.
[84] C.E. Powell, M.P. Cifuentes, J.P. Morrall, R. Stranger, M.G. Humphrey, M. Samoc, B. Luther-Davies, G.A. Heath, J. Am. Chem. Soc. 125 (2003) 602.
[85] A. Dahan, A. Weissberg, M. Portnoy, Chem. Commun. (2003) 1206.
[86] N.E. Leadbeater, M. Marco, Chem. Rev. 102 (2002) 3217, and references cited therein.
[87] For an example see: S.T. Nguyen, R.H. Grubbs, J. Organometal. Chem. 497 (1995) 195.
[88] Dendrimers of various types and generation are commercially available. Dendritic NanoTechnologies (www.dnanotech.com) offer a wide variety of PAMAM type dendrimers, for example. In addition, first to fifth generation DAB-amine dendrimers are listed in the 2003–2004 catalogue of the Aldrich Chemical Co.